

Joint Active and Passive Beamforming Design for IRS-aided MIMO ISAC Based on Sensing Mutual Information

Jin Li, Gui Zhou, *Member, IEEE*, Tantaog Gong, Nan Liu, and Rui Zhang, *Fellow, IEEE*

Abstract—In this paper, we investigate the intelligent reflecting surface (IRS)/reconfigurable intelligent surface (RIS)-aided integrated sensing and communication (ISAC) system based on sensing mutual information (MI). Specifically, the base station (BS) perceives the sensing target via the reflected sensing signal by the IRS, while communicating with the users simultaneously. Our aim is to maximize the sensing MI, subject to the quality of service (QoS) constraints for all communication users, the transmit power constraint at the BS, and the unit-modulus constraint on the IRS's passive reflection. We solve this problem under two cases: one simplified case assuming a line-of-sight (LoS) channel between the BS and IRS and no clutter interference to sensing, and the other generalized case considering the Rician fading channel of the BS-IRS link and the presence of clutter interference to sensing. For the first case, we show that the dedicated sensing beamformer cannot enhance the sensing MI if the BS-user direct links are blocked, and develop a low-complexity iterative algorithm to jointly optimize the BS and IRS active/passive beamformers. In contrast, for the second case, we propose an alternative iterative algorithm, which can also be applied to the first case, to solve the beamforming design problem under the general setup. Numerical results are provided to validate the performance of the proposed algorithms, as compared to various benchmark schemes.

Index Terms—Integrated sensing and communication (ISAC), intelligent reflecting surface (IRS), reconfigurable intelligent surface (RIS), sensing mutual information, beamforming, majorization-minimization (MM).

I. INTRODUCTION

The next generation (6G) wireless networks with both high-accuracy sensing and high-quality communication are expected to support various applications more capably, such as environmental monitoring, smart home, vehicle to everything (V2X) communication and industrial internet of things (IoT) [1]–[4]. In the existing literature, there are two general approaches to co-design sensing and communication systems: radar communication co-existence (RCC) and integrated sensing and communication (ISAC) [2]. RCC systems allocate the spectrum resource for sensing and communication appropriately to achieve their co-existence and reduce mutual

interference [5]. By comparison, ISAC systems, also called dual-functional radar and communication (DFRC) or joint radar and communication (JRC) systems, can obtain integration and coordination gains by forming a unified system with shared spectrum, energy and hardware [2], [3]. On the other hand, multiple-input multiple-output (MIMO), which can greatly improve the sensing performance compared with traditional phase-array radar and effectively compensate the high path-loss and attenuation of millimeter wave (mm-Wave) communications [6], [7], has been widely applied in ISAC systems [8], [9]. However, the energy consumption and hardware complexity of MIMO systems can go up drastically with the increasing number of antennas equipped due to their associated radio frequency (RF) chains. Thus, intelligent reflecting surface (IRS)/reconfigurable intelligent surface (RIS) has been recognized as a promising technology for MIMO in 6G, which can offer the same performance advantages of conventional MIMO but is more cost-effective due to the use of passive reflection elements only [10]. In communication systems, IRS can greatly boost the communication performance by creating a reflected communication link in addition to the direct communication link [10], [11]. Furthermore, in a non-favorable environment for sensing where the direct sensing link between the base station (BS) and the sensing target is blocked by obstacles [12], IRS can still assist in the sensing task via the reflected link. Therefore, IRS can be used to further improve the performance of MIMO ISAC systems.

There are many prior works on IRS-aided MIMO sensing [13], [14] and MIMO ISAC systems, where the sensing performance is measured by different metrics, such as signal-to-interference-plus-noise-ratio (SINR), detection probability, beam pattern, or Cramér-Rao bound (CRB) [6]. In [15]–[19], the sensing SINR was adopted to design the ISAC beamforming of the BS and the passive beamforming of the IRS while the communication performance is satisfied. The authors in [20] and [21] studied the target detection probability and proposed IRS-aided ISAC beamforming design by maximizing the communication signal-to-noise-ratio (SNR) or minimizing the weighted communication mean square error (MSE) under a minimum detection probability constraint. Song *et al.* considered the CRB of non-line-of-sight (NLoS) sensing link in the IRS-aided ISAC system and derived the estimation CRB [22]. Beamforming design for IRS-aided sensing based on beam pattern metric was also studied in [23]–[26].

Mutual information (MI) is another important sensing performance metric. Some existing works have exhibited the

This article was presented in part at the IEEE PIMRC 2024.

J. Li, T. Gong and N. Liu are with the National Mobile Communications Research Laboratory, Southeast University, Nanjing 211189, China. (e-mail: lijn, gongtantaog, nanliu@seu.edu.cn). G. Zhou is with the Institute for Digital Communications, Friedrich-Alexander-University Erlangen-Nürnberg (FAU), 91054 Erlangen, Germany (email: gui.zhou@fau.de). R. Zhang is with School of Science and Engineering, Shenzhen Research Institute of Big Data, The Chinese University of Hong Kong, Shenzhen, Guangdong 518172, China (e-mail: rzhang@cuhk.edu.cn). He is also with the Department of Electrical and Computer Engineering, National University of Singapore, Singapore 117583 (e-mail: elezhang@nus.edu.sg).

benefits of waveform design based on MI and derived its fundamental performance limits. In radar systems, when the target response matrix is drawn according to Gaussian distribution, waveform design with higher sensing MI between the target response matrix and the echo signal can achieve better radar classification and estimation performance [27]. Furthermore, compared to phase array radar, MIMO radar can co-exist with communication systems more efficiently by using waveform design based on sensing MI [28]. Additionally, in MIMO ISAC systems, sensing MI can provide a universal lower bound for some sensing distortion metrics, such as detection probability and MSE [29]. In [30], it was shown that MIMO ISAC beamforming scheme based on sensing MI metric can suppress the clutter interference effectively and attain better transmit beampattern and root mean square error (RMSE) of angle estimation compared with MIMO ISAC beamforming schemes based on CRB and beampattern metrics. Several recent works also adopted sensing MI metric to measure the sensing performance in IRS-aided MIMO ISAC systems. Under the assumption that IRS works as a colocated MIMO radar with compact antenna spacing for the sensing task, Zhang *et al.* proposed an iterative algorithm based on manifold optimization by maximizing the weighted sum of communication rate and sensing MI to optimize the overall IRS-assisted MIMO ISAC performance [31]. In contrast, the authors in [32] considered the situation where IRS works as a statistical MIMO radar with widely separated antennas such that the correlations between different columns of the target response matrix can be neglected [33]. In this case, they deduced that the sensing MI cannot be affected by the reflection coefficients matrix of the IRS and proposed the corresponding transmit beamforming and IRS reflective beamforming schemes by maximizing the weighted sum of communication rate and sensing MI.

Different from the above works, this paper considers an IRS-aided MIMO ISAC system where the IRS, regarded as a colocated MIMO radar with compact antenna spacing, serves both sensing and communication tasks. In particular, we consider the practically challenging scenario where the direct sensing link from the BS to the sensing target is blocked by obstacles, such as buildings, and thus the IRS is deployed to create a reflected sensing link to bypass the obstacles [34]. Under this setup, sensing MI is adopted as the performance metric for the sensing task. In contrast to the existing works which designed the IRS-aided ISAC system by only considering the overall performance, e.g., maximizing the weighted sum of communication rate and sensing MI [31], this paper considers the scenario when the quality of service (QoS) requirements need to be guaranteed for all communication users and the sensing is subjected to the clutter interference in a non-favorable environment. Furthermore, instead of utilizing IRS as a statistical MIMO radar in [32], IRS is used as a colocated MIMO radar in this paper and the sensing MI is linked with the reflection coefficients matrix of the IRS in a different way.

The main contributions of this paper are summarized as follows:

- In this paper, we aim to maximize the sensing MI, subject

to the QoS constraints for all communication users, the transmit power constraint at the BS and the unit-modulus constraint on the IRS's passive reflection. The BS transmit beamformer and IRS reflection coefficients are jointly optimized. More specifically, we consider two cases: one simplified case considering a line-of-sight (LoS) BS-IRS channel and no clutter interference to sensing, and the other generalized case with a Rician fading NLoS BS-IRS channel and the presence of clutter interference to sensing.

- In the simplified case, the nonconvex sensing MI is firstly simplified by exploring the rank-one property of the LoS BS-IRS channel. Then, contrary to the general result that dedicated sensing beamformer usually enhances sensing MI, we show that it cannot improve the sensing MI in our considered system if the direct channels between the BS and communication users are completely obstructed. Besides, we propose a low-complexity iterative algorithm to solve the formulated problem, where semidefinite relaxation (SDR), rank-1 projection, eigenvalue decomposition (EVD), and convex-concave procedure (CCP) methods are adopted to solve the problem efficiently.

- In the generalized case, the majorization-minimization (MM) method is applied to approximate the intractable non-convex objective function as a biconcave minorizer. Then, an alternative iterative algorithm, which can also be applicable to the simplified case, is proposed for this general setup based on various methods, such as matrix transformations, SDR and Gaussian randomization.

- Numerical results validate that, in the simplified case, the proposed low-complexity iterative algorithm has lower computational time and better performance as compared to the proposed alternative iterative algorithm for the generalized case. Moreover, in scenarios with LoS BS-IRS channel, the beampattern performance may be worse compared to scenarios with a Rician fading channel for the BS-IRS link, as the BS cannot sense all directions of the extended sensing target in the former case. Furthermore, compared with other benchmarks, our proposed algorithms can achieve superior performance in terms of both sensing MI and beampattern.

The rest of this paper is organized as follows. Section II introduces the system model and derives the closed-form expression of sensing MI. The optimization problems for the simplified case and the generalized case are respectively investigated in Sections III and IV. Numerical results and conclusions are provided in Sections V and VI, respectively.

Notations: The following mathematical notations are adopted throughout this paper. Scalars, vectors, and matrices are denoted by normal font, boldface lowercase letters, and boldface uppercase letters, respectively. The symbols \mathbf{A}^T , \mathbf{A}^* , \mathbf{A}^H , and \mathbf{A}^{-1} represent the transpose, conjugate, hermitian, and inverse operations of matrix \mathbf{A} , respectively. The l_2 norm of vector \mathbf{a} is denoted by $\|\mathbf{a}\|$, and the Frobenius norm of matrix \mathbf{A} is denoted by $\|\mathbf{A}\|_F$. The symbols $\det(\mathbf{A})$, $\text{Tr}(\mathbf{A})$, and $\text{Re}(\mathbf{A})$ represents the determinant, trace, and real part of a matrix, respectively. Complex field, real field, and the imaginary unit are denoted as \mathbb{C} , \mathbb{R} , and $j = \sqrt{-1}$, respectively. $|a|$ and $\angle a$ denote the modulus and angle of complex number a , respectively. $\lambda_{\min}(\mathbf{A})$ represents the minimum

eigenvalue of matrix \mathbf{A} . $[\mathbf{A}]_{p:q,m:n}$ denotes a matrix with elements being the p -th to the q -th rows and the m -th to the n -th columns of matrix \mathbf{A} , and $[\mathbf{a}]_m$ denotes the m -th element of vector \mathbf{a} . The Kronecker product and Hadamard product between matrices \mathbf{X} and \mathbf{Y} are respectively denoted by $\mathbf{X} \otimes \mathbf{Y}$ and $\mathbf{X} \circ \mathbf{Y}$. $\text{diag}(\mathbf{a})$ represents the diagonal matrix with the main diagonal elements being the entries of vector \mathbf{a} , and $\text{Diag}(\mathbf{A})$ denotes the vector with entries from the main diagonal elements of matrix \mathbf{A} . The vectorization of matrix \mathbf{A} is represented by $\text{vec}(\mathbf{A})$, and $\text{unvec}_{N,N}(\mathbf{a})$ denotes undo the vectorization, i.e., matrixizing a vector \mathbf{a} into an $N \times N$ matrix. Complex Gaussian distribution is denoted by \mathcal{CN} , \mathbf{I}_a denotes the identity matrix of size a , $\mathbf{0}_{a \times b}$ denotes the matrix of size $a \times b$ with every element being 0, and $\mathbf{1}_a$ represents the column vector of size a with every element being 1.

II. SYSTEM MODEL

As shown in Fig. 1, we consider an IRS-aided ISAC system, where a MIMO DFRC BS equipped with an N -antenna uniform linear array (ULA) senses a radar target and transmits information to K single-antenna communication users simultaneously, and an IRS equipped with a M -reflecting-element ULA is deployed to assist in both sensing and communication. We assume that the direct sensing link between the BS and the radar target is severely blocked by obstacles, and as a result, the BS working as a monostatic radar can only sense the radar target via the reflected sensing link created by the IRS.

The degrees-of-freedom (DoFs) of the conventional communication-only beamformer is at most the number of users if $K \leq N$, which may degrade the sensing performance [35]. To fully exploit the DoFs of the transmit signals, we introduce dedicated sensing beamformers for target sensing in addition to communication beamformers to further improve the sensing performance [8], [35]. Thus, the transmit DFRC signal at the BS is given by

$$\mathbf{X} = \mathbf{W}\mathbf{S} = [\mathbf{W}_C \quad \mathbf{W}_R] \begin{bmatrix} \mathbf{S}_C \\ \mathbf{S}_R \end{bmatrix} \in \mathbb{C}^{N \times L},$$

where $\mathbf{W} \in \mathbb{C}^{N \times (K+N)}$ is the dual-functional beamforming matrix at the BS with $\mathbf{W}_C = [\mathbf{w}_1, \mathbf{w}_2, \dots, \mathbf{w}_K] \in \mathbb{C}^{N \times K}$ and $\mathbf{W}_R \in \mathbb{C}^{N \times N}$ being the beamforming matrices for communication and sensing, respectively, and $\mathbf{S} \in \mathbb{C}^{(K+N) \times L}$ is the signal matrix with $\mathbf{S}_C \in \mathbb{C}^{K \times L}$ and $\mathbf{S}_R \in \mathbb{C}^{N \times L}$ being K communication signals intended for K users and dedicated probing signals for target sensing, respectively. Here, L is the length of communication time slots as well as the number of radar fast-time snapshots. Throughout this paper, we assume that $K \leq N \leq L$ for the purpose of exposition [8]. Additionally, we assume that each entry in \mathbf{S}_C is i.i.d, and follows the complex Gaussian distribution with zero mean and unit variance, and \mathbf{S}_R is generated by pseudo random coding and orthogonal to \mathbf{S}_C [8], [35]. Therefore, according to the law of large numbers, if L is asymptotically large, we have $\frac{1}{L}\mathbf{S}_R\mathbf{S}_R^H \approx \mathbf{I}_N$, $\frac{1}{L}\mathbf{S}_C\mathbf{S}_C^H \approx \mathbf{I}_K$, and $\frac{1}{L}\mathbf{S}_C\mathbf{S}_R^H = \mathbf{0}_{K \times N}$. Based on the assumptions above, the following condition holds:

$$\frac{1}{L}\mathbf{S}\mathbf{S}^H \approx \mathbf{I}_{K+N}. \quad (1)$$

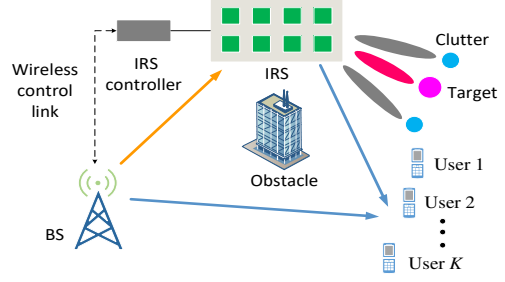


Fig. 1: An IRS-aided ISAC system.

The reflection coefficients matrix of the IRS is represented by $\mathbf{E} = \text{diag}(e_1, e_2, \dots, e_M) \in \mathbb{C}^{M \times M}$, where $|e_m|^2 = 1, m = 1, \dots, M$. In addition, the channels between the BS and the IRS, the IRS and the k -th user, and the BS and the k -th user are denoted by $\mathbf{H}_{\text{BI}} \in \mathbb{C}^{M \times N}$, $\mathbf{h}_{\text{IU},k} \in \mathbb{C}^{M \times 1}$, and $\mathbf{h}_{\text{BU},k} \in \mathbb{C}^{N \times 1}$, respectively. It is assumed that perfect channel state information (CSI) for the above communication links is known at the BS, such that the BS designs the beamforming matrix and the reflection coefficients matrix of the IRS jointly, while the latter is sent to the IRS controller via a wireless control link as shown in Fig. 1 for implementation [10].

A. Communication Model

The received signal at the k -th user in the l -th time slot can be written as

$$y_{k,l} = (\mathbf{h}_{\text{BU},k}^H + \mathbf{h}_{\text{IU},k}^H \mathbf{E} \mathbf{H}_{\text{BI}}) \mathbf{x}_l + n_{k,l}, \quad (2)$$

where $n_{k,l}$ is the additive white Gaussian noise (AWGN) following distribution $n_{k,l} \sim \mathcal{CN}(0, \sigma_k^2)$.

Then, the achievable rate of the k -th user is given by

$$R_k = \log_2 \left(1 + \frac{|\mathbf{h}_k^H \mathbf{w}_k|^2}{\sum_{i=1, i \neq k}^K |\mathbf{h}_k^H \mathbf{w}_i|^2 + \|\mathbf{h}_k^H \mathbf{W}_R\|_2^2 + \sigma_k^2} \right), \quad (3)$$

where $\mathbf{h}_k^H = \mathbf{h}_{\text{BU},k}^H + \mathbf{h}_{\text{IU},k}^H \mathbf{E} \mathbf{H}_{\text{BI}}$. Note that although the dedicated sensing beamforming \mathbf{W}_R may improve the sensing performance, it can also cause the interference for communication SINR in (3), which deteriorates the communication performance.

B. Radar/Sensing Model

In the following, as shown in Fig. 1, the clutter interference caused by scatterers around the radar target is considered [36]. Thus, the echo signal received at the BS can be written as

$$\mathbf{Y}_R = \mathbf{H}_{\text{BI}}^H \mathbf{E}^H (\mathbf{G}_R + \mathbf{G}_C) \mathbf{E} \mathbf{H}_{\text{BI}} \mathbf{X} + \mathbf{Z}_R, \quad (4)$$

where $\mathbf{G}_R \in \mathbb{C}^{M \times M}$ is the target response matrix, $\mathbf{G}_C \in \mathbb{C}^{M \times M}$ is the interference response matrix, and \mathbf{Z}_R is the AWGN matrix with each entry of \mathbf{Z}_R being i.i.d, and following the complex Gaussian distribution with zero mean and variance σ_R^2 , i.e., $\text{vec}(\mathbf{Z}_R^H) \sim \mathcal{CN}(\mathbf{0}, \sigma_R^2 \mathbf{I}_{NL})$.

By vectorizing \mathbf{Y}_R^H , we have

$$\mathbf{y}_R = \text{vec}(\mathbf{Y}_R^H)$$

$$= [(\mathbf{H}_{\text{BI}}^T \mathbf{E}^T) \otimes (\mathbf{X}^H \mathbf{H}_{\text{BI}}^H \mathbf{E}^H)](\mathbf{g}_R + \mathbf{g}_C) + \mathbf{z}_R, \quad (5)$$

where $\mathbf{g}_R = \text{vec}(\mathbf{G}_R^H)$, $\mathbf{g}_C = \text{vec}(\mathbf{G}_C^H)$ and $\mathbf{z}_R = \text{vec}(\mathbf{Z}_R^H)$. We assume that \mathbf{g}_R and \mathbf{g}_C follow the complex Gaussian distribution, i.e., $\mathbf{g}_R \sim \mathcal{CN}(\mathbf{0}, \mathbf{R}_R)$ and $\mathbf{g}_C \sim \mathcal{CN}(\mathbf{0}, \mathbf{R}_C)$. We also assume that \mathbf{g}_R , \mathbf{g}_C , and \mathbf{z}_R are independent to each other.

In order to calculate the covariance matrix \mathbf{R}_R , we first introduce the model of target response matrix \mathbf{G}_R . We assume that IRS works as a monostatic colocated MIMO radar [6], [12], i.e., the angle of arrival (AOA) is equal to the angle of departure (AOD). Hence, according to the Swerling target models, the target response matrix \mathbf{G}_R can be expressed as [28], [37]

$$\mathbf{G}_R = \sum_{p=1}^{N_r} \alpha_p^r \mathbf{b}(\theta_p^r) \mathbf{b}^H(\theta_p^r), \quad (6)$$

where N_r is the number of scatterers, θ_p^r is the AOA/AOD of the p -th scatterer relative to the IRS, α_p^r is the complex amplitude of the p -th scatterer containing the round-trip pathloss and the radar cross section of the scatterer, and $\mathbf{b}(\theta) \in \mathbb{C}^{M \times 1}$ is the steering vector of the IRS. Here, the radar target is considered as an extended target which is a sum of multiple point scatterers, i.e., $N_r > 1$ [8], [27]. The point target is a special case of an extended target when the target is far away from the IRS, i.e., $N_r = 1$ [8], [38].

With the target response matrix (6), the covariance matrix \mathbf{R}_R is given by

$$\begin{aligned} \mathbf{R}_R &= \mathbb{E}(\mathbf{g}_R \mathbf{g}_R^H) \\ &= \sum_{p=1}^{N_r} \beta_p^2 (\mathbf{b}^*(\theta_p^r) \otimes \mathbf{b}(\theta_p^r)) (\mathbf{b}^*(\theta_p^r) \otimes \mathbf{b}(\theta_p^r))^H, \end{aligned} \quad (7)$$

where $\beta_p^2 = \mathbb{E}(\alpha_p^r \alpha_p^{r,*})$.

We consider that the clutter interference is resulted from many scatterers around the radar target. Similar to (6), (7), the interference response matrix \mathbf{G}_C and its covariance matrix \mathbf{R}_C can be respectively written as

$$\begin{aligned} \mathbf{G}_C &= \sum_{q=1}^{N_c} \alpha_q^c \mathbf{b}(\theta_q^c) \mathbf{b}^H(\theta_q^c), \quad (8) \\ \mathbf{R}_C &= \mathbb{E}(\mathbf{g}_C \mathbf{g}_C^H) \\ &= \sum_{q=1}^{N_c} \gamma_q^2 (\mathbf{b}^*(\theta_q^c) \otimes \mathbf{b}(\theta_q^c)) (\mathbf{b}^*(\theta_q^c) \otimes \mathbf{b}(\theta_q^c))^H, \end{aligned} \quad (9)$$

where $\gamma_q^2 = \mathbb{E}(\alpha_q^c \alpha_q^{c,*})$, N_c is the number of interfering scatterers, α_q^c is the complex amplitude of the q -th interfering scatterer, and θ_q^c is the AOA/AOD of the q -th interfering scatterer relative to the IRS.

To evaluate the sensing performance, the MI between the object parameter vector \mathbf{g}_R containing the desired parameters and the measurement vector \mathbf{y}_R is adopted as the sensing performance metric [27]. Then, according to the aforementioned assumptions, the channel between the BS and the IRS, \mathbf{H}_{BI} , the reflection coefficients matrix, \mathbf{E} , and the transmit signal at

the BS, \mathbf{X} , are known at the DFRC BS. Hence, given \mathbf{H}_{BI} , \mathbf{E} , and \mathbf{X} , the MI between \mathbf{y}_R and \mathbf{g}_R can be written as [28]

$$\begin{aligned} &\mathcal{I}(\mathbf{y}_R; \mathbf{g}_R | \mathbf{X}, \mathbf{H}_{\text{BI}}, \mathbf{E}) \\ &= \mathcal{H}(\mathbf{y}_R | \mathbf{X}, \mathbf{H}_{\text{BI}}, \mathbf{E}) - \mathcal{H}(\mathbf{y}_R | \mathbf{g}_R, \mathbf{X}, \mathbf{H}_{\text{BI}}, \mathbf{E}) \\ &= - \int p(\mathbf{y}_R | \mathbf{X}, \mathbf{H}_{\text{BI}}, \mathbf{E}) \log p(\mathbf{y}_R | \mathbf{X}, \mathbf{H}_{\text{BI}}, \mathbf{E}) \\ &\quad + \int p(\mathbf{y}_R | \mathbf{g}_R, \mathbf{X}, \mathbf{H}_{\text{BI}}, \mathbf{E}) \log p(\mathbf{y}_R | \mathbf{g}_R, \mathbf{X}, \mathbf{H}_{\text{BI}}, \mathbf{E}), \\ &= \log [\det ((\mathbf{I}_N \otimes \mathbf{X}^H) \mathbf{A} \mathbf{R}_{RC} \mathbf{A}^H (\mathbf{I}_N \otimes \mathbf{X}) + \sigma_R^2 \mathbf{I}_{LN})] \\ &\quad - \log [\det ((\mathbf{I}_N \otimes \mathbf{X}^H) \mathbf{A} \mathbf{R}_C \mathbf{A}^H (\mathbf{I}_N \otimes \mathbf{X}) + \sigma_R^2 \mathbf{I}_{LN})], \quad (10) \\ &\approx \log [\det (\frac{L}{\sigma_R^2} \widetilde{\mathbf{W}} \mathbf{A} \mathbf{R}_{RC} \mathbf{A}^H \widetilde{\mathbf{W}}^H + \mathbf{I}_{N(K+N)})] \\ &\quad - \log [\det (\frac{L}{\sigma_R^2} \widetilde{\mathbf{W}} \mathbf{A} \mathbf{R}_C \mathbf{A}^H \widetilde{\mathbf{W}}^H + \mathbf{I}_{N(K+N)})], \quad (11) \end{aligned}$$

where $\mathcal{H}(\cdot)$ denotes the differential entropy, $p(\cdot)$ represents the probability distribution function (PDF), $\mathbf{A} = \mathbf{H}_{\text{BI}}^T \mathbf{E}^T \otimes \mathbf{H}_{\text{BI}}^H \mathbf{E}^H$, $\widetilde{\mathbf{W}} = \mathbf{I}_N \otimes \mathbf{W}^H$, $\mathbf{R}_{RC} = \mathbf{R}_R + \mathbf{R}_C$, (11) follows the properties of determinant $\det(\mathbf{I}_a + \mathbf{A}\mathbf{B}) = \det(\mathbf{I}_b + \mathbf{B}\mathbf{A})$, $\det(c\mathbf{A}) = c^a \det(\mathbf{A})$ [39], and the condition (1) with sufficiently large L .

In the following, we discuss two cases separately: one is the simplified case with the LoS BS-IRS channel and no clutter interference to sensing, while the other one is the generalized case with the Rician BS-IRS channel and the presence of clutter interference to sensing.

III. THE SIMPLIFIED CASE: LOS BS-IRS CHANNEL AND NO CLUTTER INTERFERENCE TO SENSING

In this section, assuming that the interfering echo signal is very weak, we can ignore the clutter interference, i.e., $\mathbf{R}_C = 0$. Additionally, if the BS and the IRS are deployed in the open space without significant scatterers, we can assume that the channel between the BS and the IRS, \mathbf{H}_{BI} , is the LoS channel [40]. As such \mathbf{H}_{BI} can be simplified as

$$\mathbf{H}_{\text{BI}} = \xi \mathbf{b}(\theta_{\text{I}}) \mathbf{a}^H(\theta_{\text{B}}), \quad (12)$$

where θ_{B} is the AOD relative to the BS, θ_{I} is the AOA relative to the IRS, $\mathbf{a}(\theta) \in \mathbb{C}^{N \times 1}$ is the transmit steering vector of the BS, and ξ is the pathloss. We aim to jointly design the BS beamforming matrix \mathbf{W} and IRS reflection coefficients matrix \mathbf{E} to maximize the sensing MI while satisfying users' individual communication rate constraints, BS's transmit power constraint and unit modulus constraints of reflection elements. Thus, by letting $\mathbf{R}_C = 0$ in (11), the optimization problem is formulated as follows:

$$\max_{\mathbf{W}, \mathbf{E}} \log [\det (\frac{L}{\sigma_R^2} \widetilde{\mathbf{W}} \mathbf{A} \mathbf{R}_R \mathbf{A}^H \widetilde{\mathbf{W}}^H + \mathbf{I}_{N(K+N)})] \quad (13a)$$

$$\text{s.t. } R_k \geq r_k, \quad \forall k, \quad (13b)$$

$$\|\mathbf{W}\|_F^2 \leq P_0, \quad (13c)$$

$$|e_m|^2 = 1, \quad m = 1, \dots, M, \quad (13d)$$

where r_k is the required communication rate of the k -th user, and P_0 is the maximum BS transmit power.

Due to the high-degree polynomial of the determinant of the matrix and coupling variables, the nonconcave objective function (13a) is difficult to tackle. Hence, we first use the rank-one property of \mathbf{H}_{BI} to transform the objective function (13a) into a tractable term.

With (12), matrix \mathbf{A} can be rewritten as

$$\mathbf{A} = (\mathbf{H}_{\text{BI}}^T \otimes \mathbf{H}_{\text{BI}}^H) \mathbf{J} = \xi^2 \bar{\mathbf{a}}(\theta_{\text{B}}) \bar{\mathbf{b}}^H(\theta_{\text{I}}) \mathbf{J}, \quad (14)$$

where $\bar{\mathbf{a}}(\theta_{\text{B}}) = (\mathbf{a}^*(\theta_{\text{B}}) \otimes \mathbf{a}(\theta_{\text{B}})) \in \mathbb{C}^{N^2 \times 1}$, $\bar{\mathbf{b}}^H(\theta_{\text{I}}) = (\mathbf{b}^T(\theta_{\text{I}}) \otimes \mathbf{b}^H(\theta_{\text{I}})) \in \mathbb{C}^{1 \times M^2}$, $\mathbf{J} = \mathbf{E}^T \otimes \mathbf{E}^H$, and the derivation of (14) follows the property of the Kronecker product $(\mathbf{A} \otimes \mathbf{C})(\mathbf{B} \otimes \mathbf{D}) = (\mathbf{AB}) \otimes (\mathbf{CD})$ [39].

Then, substituting matrix \mathbf{A} in (13a) with (14) and using the property of determinant $\det(\mathbf{I}_a + \mathbf{AB}) = \det(\mathbf{I}_b + \mathbf{BA})$, the objective function (13a) can be transformed as

$$\log \left[\det \left(\frac{L \xi^4}{\sigma_{\text{R}}^2} \bar{\mathbf{b}}^H(\theta_{\text{I}}) \mathbf{J} \mathbf{R}_{\text{R}} \mathbf{J}^H \bar{\mathbf{b}}(\theta_{\text{I}}) \bar{\mathbf{a}}^H(\theta_{\text{B}}) \widetilde{\mathbf{W}}^H \widetilde{\mathbf{W}} \bar{\mathbf{a}}(\theta_{\text{B}}) + 1 \right) \right]. \quad (15)$$

Hence, with (15), Problem (13) can be simplified as

$$\begin{aligned} \max_{\mathbf{W}, \mathbf{E}} \quad & \bar{\mathbf{b}}^H(\theta_{\text{I}}) \mathbf{J} \mathbf{R}_{\text{R}} \mathbf{J}^H \bar{\mathbf{b}}(\theta_{\text{I}}) \bar{\mathbf{a}}^H(\theta_{\text{B}}) \widetilde{\mathbf{W}}^H \widetilde{\mathbf{W}} \bar{\mathbf{a}}(\theta_{\text{B}}) \\ \text{s.t.} \quad & (13\text{b}), (13\text{c}), (13\text{d}). \end{aligned} \quad (16\text{a}) \quad (16\text{b})$$

Next, in order to address the coupling variables, we resort to an alternating optimization (AO) algorithm to solve Problem (16) in the following.

A. BS Beamforming Matrix Optimization

In this subsection, we optimize the BS beamforming matrix \mathbf{W} when \mathbf{E} is fixed. Note that, given \mathbf{E} , the term $\bar{\mathbf{b}}^H(\theta_{\text{I}}) (\mathbf{E}^T \otimes \mathbf{E}^H) \mathbf{R}_{\text{R}} (\mathbf{E}^* \otimes \mathbf{E}) \bar{\mathbf{b}}(\theta_{\text{I}})$ in (16a) is a scalar. Thus, maximizing (13a) is equivalent to maximizing $\bar{\mathbf{a}}^H(\theta_{\text{B}}) \widetilde{\mathbf{W}}^H \widetilde{\mathbf{W}} \bar{\mathbf{a}}(\theta_{\text{B}})$, and this equation can be further transformed as

$$\begin{aligned} & (\mathbf{a}^T(\theta_{\text{B}}) \mathbf{a}^*(\theta_{\text{B}})) \otimes (\mathbf{a}^H(\theta_{\text{B}}) \mathbf{W} \mathbf{W}^H \mathbf{a}(\theta_{\text{B}})) \\ & = N \mathbf{a}^H(\theta_{\text{B}}) \mathbf{W} \mathbf{W}^H \mathbf{a}(\theta_{\text{B}}), \end{aligned} \quad (17)$$

where the derivation of (17) follows the property of Kronecker product $(\mathbf{AB}) \otimes (\mathbf{CD}) = (\mathbf{A} \otimes \mathbf{C})(\mathbf{B} \otimes \mathbf{D})$ and the equality $\mathbf{a}^T(\theta_{\text{B}}) \mathbf{a}^*(\theta_{\text{B}}) = N$.

Then, we let $\mathbf{C}_{\text{X}} = \mathbf{W} \mathbf{W}^H$ and $\mathbf{W}_{\text{R}} \mathbf{W}_{\text{R}}^H = \mathbf{C}_{\text{X}} - \sum_{k=1}^K \mathbf{W}_k$, where $\mathbf{W}_k = \mathbf{w}_k \mathbf{w}_k^H$, $k = 1, \dots, K$. We also let $\mathbf{h}_k^H = \mathbf{h}_{\text{BU},k}^H + \mathbf{h}_{\text{IU},k}^H \mathbf{E} \mathbf{H}_{\text{BI}}$ and $\Omega_k = 2^{r_k} - 1$, $k = 1, \dots, K$. By using SDR and dropping rank-1 constraints [41], the optimization subproblem of Problem (16) corresponding to the BS beamforming matrix \mathbf{W} can be reformulated as an semidefinite programming (SDP) problem given by

$$\max_{\mathbf{C}_{\text{X}}, \mathbf{W}_1, \dots, \mathbf{W}_K} \quad \mathbf{a}^H(\theta_{\text{B}}) \mathbf{C}_{\text{X}} \mathbf{a}(\theta_{\text{B}}) \quad (18\text{a})$$

$$\text{s.t.} \quad \begin{aligned} & \Omega_k \text{Tr}(\mathbf{h}_k \mathbf{h}_k^H \mathbf{C}_{\text{X}}) - (1 + \Omega_k) \text{Tr}(\mathbf{h}_k \mathbf{h}_k^H \mathbf{W}_k) \\ & + \Omega_k \sigma_k^2 \leq 0, \quad \forall k, \end{aligned} \quad (18\text{b})$$

$$\text{Tr}(\mathbf{C}_{\text{X}}) \leq P_0, \quad (18\text{c})$$

$$\mathbf{C}_{\text{X}} \succeq \sum_{k=1}^K \mathbf{W}_k, \quad \mathbf{W}_k \succeq 0, \quad \forall k. \quad (18\text{d})$$

The problem above is a standard SDP problem which can be solved using CVX.

The fact that there always exists a globally optimal rank-1 solution for Problem (18) is given by the following theorem.

Theorem 1 *The globally optimal rank-1 solution to Problem (18) is*

$$\hat{\mathbf{C}}_{\text{X}} = \tilde{\mathbf{C}}_{\text{X}}, \quad \hat{\mathbf{W}}_k = \hat{\mathbf{w}}_k \hat{\mathbf{w}}_k^H, \quad (19)$$

for $k = 1, \dots, K$, where $\tilde{\mathbf{C}}_{\text{X}}$ and $\tilde{\mathbf{W}}_k$ are the optimal solutions to Problem (18), and $\hat{\mathbf{w}}_k = (\mathbf{h}_k^H \tilde{\mathbf{W}}_k \mathbf{h}_k)^{-\frac{1}{2}} \tilde{\mathbf{W}}_k \mathbf{h}_k$.

Proof: See [35, Appendix A]. \blacksquare

Upon getting the optimal $\hat{\mathbf{C}}_{\text{X}}$ and $\hat{\mathbf{W}}_k$ from Theorem 1, we can adopt eigenvalue decomposition or Cholesky decomposition to obtain the optimal $\hat{\mathbf{W}}_{\text{R}}$. Next, the following lemma states the conditions under which the dedicated sensing beamformer cannot improve the sensing MI.

Lemma 1 *The dedicated sensing beamformer cannot improve the sensing MI if the BS-user links are completely blocked, i.e., $\mathbf{a}^H(\theta_{\text{B}}) \sum_{k=1}^K \tilde{\mathbf{W}}_k \mathbf{a}(\theta_{\text{B}}) \leq \mathbf{a}^H(\theta_{\text{B}}) (\sum_{k=1}^K \hat{\mathbf{W}}_k + \hat{\mathbf{C}}_{\text{R}}) \mathbf{a}(\theta_{\text{B}})$, with equality if $\mathbf{h}_{\text{BU},k} = 0$ and the LoS BS-IRS channel given in (12), where $\tilde{\mathbf{W}}_k$ is the rank-1 solution obtained by Theorem 1 to the communication-only beamforming problem, $\hat{\mathbf{W}}_k$ and $\hat{\mathbf{C}}_{\text{R}}$ are the rank-1 optimal solutions to Problem (18).*

Proof: See Appendix A. \blacksquare

B. IRS Reflection Coefficients Optimization

In this subsection, given \mathbf{W} , the optimization subproblem of Problem (16) corresponding to IRS reflection coefficients matrix \mathbf{E} can be reformulated as

$$\min_{\mathbf{E}} \quad -\bar{\mathbf{b}}^H(\theta_{\text{I}}) (\mathbf{E}^T \otimes \mathbf{E}^H) \mathbf{R}_{\text{R}} (\mathbf{E}^* \otimes \mathbf{E}) \bar{\mathbf{b}}(\theta_{\text{I}}) \quad (20\text{a})$$

$$\text{s.t.} \quad (13\text{b}), (13\text{d}). \quad (20\text{b})$$

Then, denoting $\mathbf{e}^H = [e_1, e_2, \dots, e_M] \in \mathbb{C}^{1 \times M}$ as the equivalent reflection coefficients vector, the communication rate constraints (13b) can be rewritten as

$$\begin{aligned} & 2\text{Re}(\mathbf{e}^H (\Omega_k \sum_{i=1, i \neq k}^K \mathbf{d}_{k,i} - \mathbf{d}_{k,k} + \Omega_k \mathbf{d}_{k,r})) + l_k \\ & + \mathbf{e}^H (\Omega_k \sum_{i=1, i \neq k}^K \mathbf{D}_{k,i} - \mathbf{D}_{k,k} + \Omega_k \mathbf{D}_{k,r}) \mathbf{e} \leq 0, \quad \forall k, \end{aligned} \quad (21)$$

where $l_k = \Omega_k \sum_{i=1, i \neq k}^K c_{k,i} + \Omega_k \sigma_k^2 - c_{k,k} + \Omega_k c_{k,r}$, $c_{k,i} = \mathbf{h}_{\text{BU},k}^H \mathbf{w}_i \mathbf{w}_i^H \mathbf{h}_{\text{BU},k}$, $c_{k,r} = \mathbf{h}_{\text{BU},k}^H \mathbf{W}_{\text{R}} \mathbf{W}_{\text{R}}^H \mathbf{h}_{\text{BU},k}$, $\mathbf{d}_{k,i} = \text{diag}(\mathbf{h}_{\text{IU},k}^H) \mathbf{H}_{\text{BI}} \mathbf{w}_i \mathbf{w}_i^H \mathbf{h}_{\text{BU},k}$, $\mathbf{d}_{k,r} = \text{diag}(\mathbf{h}_{\text{IU},k}^H) \mathbf{H}_{\text{BI}} \mathbf{W}_{\text{R}} \mathbf{W}_{\text{R}}^H \mathbf{h}_{\text{BU},k}$, $\mathbf{D}_{k,i} = \text{diag}(\mathbf{h}_{\text{IU},k}^H) \mathbf{H}_{\text{BI}} \mathbf{w}_i \mathbf{w}_i^H \mathbf{H}_{\text{BI}}^H \text{diag}(\mathbf{h}_{\text{IU},k}^H)^H$, and $\mathbf{D}_{k,r} = \text{diag}(\mathbf{h}_{\text{IU},k}^H) \mathbf{H}_{\text{BI}} \mathbf{W}_{\text{R}} \mathbf{W}_{\text{R}}^H \mathbf{H}_{\text{BI}}^H \text{diag}(\mathbf{h}_{\text{IU},k}^H)^H$.

In order to transform the nonconvex constraints (21) into convex constraints, EVD and the equation $\mathbf{e}^H \mathbf{e} = M$ are applied, and then (21) can be further expressed as

$$\mathbf{e}^H \widetilde{\mathbf{F}}_k \mathbf{e} + \lambda_{\min}(\mathbf{F}_k) M + 2\text{Re}(\mathbf{e}^H \bar{\mathbf{d}}_k) + l_k \leq 0, \quad \forall k, \quad (22)$$

where $\bar{\mathbf{d}}_k = \Omega_k \sum_{i=1, i \neq k}^K \mathbf{d}_{k,i} - \mathbf{d}_{k,k} + \Omega_k \mathbf{d}_{k,r}$, $\widetilde{\mathbf{F}}_k = \mathbf{F}_k - \lambda_{\min}(\mathbf{F}_k) \mathbf{I}_M$, $\widetilde{\mathbf{F}}_k \succeq \mathbf{0}$ and $\mathbf{F}_k = \Omega_k \sum_{i=1, i \neq k}^K \mathbf{D}_{k,i} - \mathbf{D}_{k,k} + \Omega_k \mathbf{D}_{k,r}$.

By taking (7) into (20a), the objective function can be rewritten as

$$\begin{aligned} & - \sum_{p=1}^{N_r} \beta_p^2 \bar{\mathbf{b}}^H(\theta_1) \check{\mathbf{E}} \check{\mathbf{E}}^H \bar{\mathbf{b}}(\theta_1) \\ & = - \sum_{p=1}^{N_r} \beta_p^2 \bar{\mathbf{b}}^H(\theta_1) \mathbf{C}_p (\mathbf{e}^* \otimes \mathbf{e}) (\mathbf{e}^T \otimes \mathbf{e}^H) \mathbf{C}_p^H \bar{\mathbf{b}}(\theta_1), \end{aligned} \quad (23a)$$

$$= -(\mathbf{e}^T \otimes \mathbf{e}^H) \mathbf{M}_R (\mathbf{e}^* \otimes \mathbf{e}), \quad (23b)$$

where $\check{\mathbf{E}} = (\mathbf{E}^T \otimes \mathbf{E}^H) (\mathbf{b}^*(\theta_p^r) \otimes \mathbf{b}(\theta_p^r))$, $\mathbf{C}_p = \text{diag}(\mathbf{b}^*(\theta_p^r)) \otimes \text{diag}(\mathbf{b}(\theta_p^r))$, $\mathbf{M}_R = \sum_{p=1}^{N_r} \beta_p^2 \mathbf{C}_p^H \bar{\mathbf{b}}(\theta_1) \bar{\mathbf{b}}^H(\theta_1) \mathbf{C}_p$, $\mathbf{M}_R \succeq \mathbf{0}$, (23a) follows the property of Kronecker product $(\mathbf{A} \otimes \mathbf{B})(\mathbf{C} \otimes \mathbf{D}) = (\mathbf{A}\mathbf{C}) \otimes (\mathbf{B}\mathbf{D})$ and the equation $\mathbf{E}^T \mathbf{b}^*(\theta) = \text{diag}(\mathbf{b}^*(\theta)) \mathbf{e}^*$.

It is challenging to deal with the nonconvex quartic objective function (23b) with respect to (w.r.t.) the optimization variable \mathbf{e} . Thus, we adopt the MM method to deal with this problem [42]. More specifically, the MM method is aimed at constructing an easy-to-solve majorizer (minorizer) for minimization (maximization) problem, where the majorizer must satisfy four conditions, i.e., (A1) – (A4), given in [11].

Based on the MM framework and second-order Taylor expansion, the upper bound of the objective function (23b) at the given point $\bar{\mathbf{e}}^{(\tau)}$ is given by

$$\begin{aligned} \bar{\mathbf{e}}^H \mathbf{M}_1 \bar{\mathbf{e}} & \leq \bar{\mathbf{e}}^H \text{Tr}(-\mathbf{M}_1) \mathbf{I}_{M^2} \bar{\mathbf{e}} + 2\text{Re}(\bar{\mathbf{e}}^H \widetilde{\mathbf{M}}_1 \bar{\mathbf{e}}^{(\tau)}) + \text{const}_1 \\ & = \text{Re}(\bar{\mathbf{e}}^H \mathbf{g}_1) + \text{const}_2, \end{aligned} \quad (24)$$

where $\mathbf{M}_1 = -\mathbf{M}_R$, $\mathbf{M}_1 \preceq \mathbf{0}$, $\bar{\mathbf{e}} = \mathbf{e}^* \otimes \mathbf{e}$, $\widetilde{\mathbf{M}}_1 = \mathbf{M}_1 - \text{Tr}(-\mathbf{M}_1) \mathbf{I}_{M^2}$, $\text{const}_1 = (\bar{\mathbf{e}}^{(\tau)})^H \widetilde{\mathbf{M}}_1 \bar{\mathbf{e}}^{(\tau)}$, $\text{const}_2 = \text{Tr}(-\mathbf{M}_1) M^2 + \text{const}_1$, $\mathbf{g}_1 = 2\widetilde{\mathbf{M}}_1 \bar{\mathbf{e}}^{(\tau)}$, the inequality follows from $\text{Tr}(-\mathbf{M}_1) \mathbf{I}_{M^2} \succeq \mathbf{M}_1$, and the equality follows from $\bar{\mathbf{e}}^H \bar{\mathbf{e}} = M^2$.

For the purpose of unifying the optimization variables, we express (24) as a function w.r.t. \mathbf{e} rather than $\bar{\mathbf{e}}$. Hence, the first term in (24) can be rewritten as

$$\text{Re}(\bar{\mathbf{e}}^H \mathbf{g}_1) = \text{Re}((\mathbf{e}^T \otimes \mathbf{e}^H) \mathbf{g}_1) = \text{Re}(\mathbf{e}^H \mathbf{G}_1 \mathbf{e}), \quad (25)$$

where $\text{vec}(\mathbf{G}_1) = \mathbf{g}_1$, and the second equality follows the property of Kronecker product $(\mathbf{C}^T \otimes \mathbf{A}) \text{vec}(\mathbf{B}) = \text{vec}(\mathbf{A}\mathbf{B}\mathbf{C})$ [39].

Although matrix $\mathbf{G}_1 \in \mathbb{C}^{M \times M}$ can be recovered by rearranging the vector $\mathbf{g}_1 \in \mathbb{C}^{M^2 \times 1}$, the computational cost for obtaining \mathbf{g}_1 is much higher compared to that for matrix \mathbf{G}_1 . Thus, the following lemma shows the mathematical expression of \mathbf{G}_1 .

Lemma 2 Matrix $\mathbf{G}_1 \in \mathbb{C}^{M \times M}$ can be written as

$$\mathbf{G}_1 = 2z_1 \mathbf{e}^{(\tau)} (\mathbf{e}^{(\tau)})^H - 2 \sum_{p=1}^{N_r} \beta_p^2 \mathbf{M}_3,$$

where $\mathbf{M}_3 = \text{diag}(\mathbf{b}(\theta_p^r))^H \mathbf{b}(\theta_1) \mathbf{b}^H(\theta_1) \text{diag}(\mathbf{b}(\theta_p^r)) \mathbf{e}^{(\tau)} (\mathbf{e}^{(\tau)})^H \text{diag}(\mathbf{b}(\theta_p^r))^H \mathbf{b}(\theta_1) \mathbf{b}^H(\theta_1) \text{diag}(\mathbf{b}(\theta_p^r))$ and $z_1 = -\text{Tr}(-\mathbf{M}_1)$.

Proof: See Appendix B. ■

Note that \mathbf{G}_1 is a Hermitian matrix, i.e., $\mathbf{e}^H \mathbf{G}_1 \mathbf{e}$ is a real number. However, \mathbf{G}_1 is a negative semidefinite matrix which

makes (25) also nonconvex. In order to address this issue, we resort to EVD, and (25) can be transformed as

$$\mathbf{e}^H \mathbf{G}_1 \mathbf{e} = \mathbf{e}^H \widetilde{\mathbf{G}}_1 \mathbf{e} + \lambda_{\min}(\mathbf{G}_1) M, \quad (26)$$

where $\widetilde{\mathbf{G}}_1 = \mathbf{G}_1 - \lambda_{\min}(\mathbf{G}_1) \mathbf{I}_M$ and $\widetilde{\mathbf{G}}_1 \succeq \mathbf{0}$.

Furthermore, by introducing nonnegative slack variable $\mathbf{f} = [f_1, f_2, \dots, f_{2M}]^T$, we can adopt penalty CCP to tackle nonconvex unit-modulus constraints (13d), which are given by [43]

$$|e_m|^2 \leq 1 + f_{M+m}, \quad m = 1, \dots, M, \quad (27)$$

$$|e_m^{(\tau)}|^2 - 2\text{Re}(e_m^* e_m^{(\tau)}) \leq f_m - 1 \quad m = 1, \dots, M. \quad (28)$$

With (22), (26), (27) and (28), Problem (20) can be recast as

$$\min_{\mathbf{e}, \mathbf{f}} \quad \mathbf{e}^H \widetilde{\mathbf{G}}_1 \mathbf{e} + \rho \sum_{i=1}^{2M} f_i \quad (29a)$$

$$\text{s.t.} \quad (22), (27), (28), \quad (29b)$$

$$f_i \geq 0, \quad i = 1, \dots, 2M, \quad (29c)$$

where ρ is the penalty parameter. Problem (29) is a convex second-order cone programming (SOCP) problem which can be solved using CVX directly.

Finally, by letting $g(\mathbf{W}, \mathbf{E})$ be the objective function value (13a), the overall algorithm for solving Problem (13) is summarized in Algorithm 1.

Algorithm 1 Low-complexity Iterative Algorithm for Solving Problem (13)

- 1: Set the outer iteration index $\kappa = 0$. Initialize $\mathbf{E}^{(0)}$ randomly, the tolerance ϵ_o , and the maximum iterations number τ_{max} .
 - 2: **repeat**
 - 3: Given $\mathbf{E}^{(\kappa)}$, solve Problem (18) and apply Theorem 1 to obtain BS beamforming matrix $\mathbf{W}^{(\kappa+1)}$.
 - 4: Set the inner iteration index $\tau = 0$. Given $\mathbf{W}^{(\kappa+1)}$, obtain $\mathbf{E}^{(\kappa+1)}$ by the following steps.
 - 5: **repeat**
 - 6: **if** $\tau < \tau_{max}$ **then**
 - 7: Solve Problem (29) to obtain $\mathbf{e}^{(\tau+1)}$.
 - 8: Update $\rho = \min(\mu\rho, \rho_{\max})$.
 - 9: Set $\tau = \tau + 1$.
 - 10: **else**
 - 11: Return to step 4 and restart the iteration with a new initial random reflection coefficients matrix.
 - 12: **end if**
 - 13: **until** $\left| \frac{g(\mathbf{W}^{(\kappa+1)}, \mathbf{E}^{(\tau+1)}) - g(\mathbf{W}^{(\kappa+1)}, \mathbf{E}^{(\tau)})}{g(\mathbf{W}^{(\kappa+1)}, \mathbf{E}^{(\tau)})} \right| \leq \epsilon_i$, $\|\mathbf{e}^{(\tau+1)} - \mathbf{e}^{(\tau)}\|_2 \leq \epsilon_d$ and $\|\mathbf{f}\|_1 \leq \epsilon_d$.
 - 14: Let $\mathbf{E}^{(\kappa+1)} = \text{diag}((\mathbf{e}^{(\tau)})^*)$ and $\kappa = \kappa + 1$.
 - 15: **until** The fractional increase of objective function value (13a) is less than ϵ_o or the iteration number is more than τ_{max} .
-

Note that the choice of ρ may affect the convergence speed of Problem (29) [43]. Thus, as shown in Step 8 of Algorithm 1, we increase the value of ρ by multiplying a ratio coefficient $\mu > 1$ in every iteration for the purpose of accelerating the

convergence. Furthermore, to avoid numerical issues, we also set an upper bound for ρ , i.e., $\rho < \rho_{\max}$. Additionally, in case that $\mathbf{E}^{(\kappa+1)}$ in Step 14 may not be feasible for Problem (20), we can restart CCP procedure in Algorithm 1 with a new random reflection coefficients matrix [43].

C. Complexity Analysis

The computational complexity of Algorithm 1 in every outer iteration is mainly due to solving the SDP problem (18) and the penalty CCP algorithm from Steps 5 to 13. The SDP problem is solved by the interior point method in CVX, and the main computational complexity of the interior point method is given by [11], [44]

$$\mathcal{O}\left(\left(\sum_{x=1}^X q_x + 2Y\right)^{\frac{1}{2}} a(a^2 + a \sum_{x=1}^X q_x^2 + \sum_{x=1}^X q_x^3 + a \sum_{y=1}^Y b_y^2)\right),$$

where a is the number of variables, X represents the number of linear matrix inequalities (LMIs) with dimension q_x , and Y denotes the number of second-order cone (SOC) constraints with dimension b_y . Problem (18) is comprised of $2K + 2$ LMIs with dimension N^2 , and the number of variables is $a_1 = N(K + N)$. Hence, the approximate complexity of solving Problem (18) is $\mathcal{O}([(2K + 2)N^2]^{\frac{1}{2}} a_1 [a_1^2 + a_1(2K + 2)N^4 + (2K + 2)N^6])$. For the penalty CCP algorithm, the major complexity depends on calculating the maximum or minimum eigenvalue in (29a) and (22) and solving SOCP problem (29). The complexity of the eigenvalue operation in the penalty CCP algorithm is $\mathcal{O}((K + 1)M^3)$. However, according to [11] and [44], the complexity of solving SOCP problem is $\mathcal{O}(UV^{3.5} + U^3V^{2.5})$, where V represents the number of SOC constraints, and the dimension of each is U . In SOCP problem (29), there are K SOC constraints with dimension M and $4M$ SOC constraints with dimension one. Therefore, the complexity of solving SOCP problem (29) per inner iteration is $\mathcal{O}(MK^{3.5} + M^3K^{2.5} + (4M)^{3.5} + (4M)^{2.5})$. Finally, supposing that the iteration number of the CCP algorithm is τ_1 , the approximate computational complexity of Algorithm 1 per outer iteration is $\mathcal{O}(\tau_1[(K + 1)M^3 + MK^{3.5} + M^3K^{2.5} + (4M)^{3.5} + (4M)^{2.5}] + [(2K + 2)N^2]^{\frac{1}{2}} a_1 [a_1^2 + a_1(2K + 2)N^4 + (2K + 2)N^6])$.

D. Convergence Analysis

Here, the convergence of Algorithm 1 is analyzed. As mentioned in [43], when the conditions in Step 13 are satisfied, i.e., $\sum_{i=1}^{2M} f_i \approx 0$, we have

$$g(\mathbf{W}^{(\kappa)}, \mathbf{E}^{(\tau)}) \leq g(\mathbf{W}^{(\kappa+1)}, \mathbf{E}^{(\tau)}) \leq g(\mathbf{W}^{(\kappa+1)}, \mathbf{E}^{(\tau+1)}),$$

where the first inequality follows the optimality of SDP problem (18), and the second inequality follows the optimality of Problem (29). Moreover, due to the bounded feasible set, the non-decreasing objective function (13a) has a finite upper bound. Therefore, the convergence of Algorithm 1 is ensured.

IV. THE GENERALIZED CASE: RICIAN BS-IRS CHANNEL AND PRESENCE OF CLUTTER INTERFERENCE TO SENSING

In this section, we consider a non-favorable propagation environment and assume that the channel between the BS and the IRS, \mathbf{H}_{BI} , is a Rician channel, and the radar clutter

interference cannot be neglected, i.e., (8) holds. Hence, the optimization problem is formulated as

$$\begin{aligned} \max_{\mathbf{W}, \mathbf{E}} \quad & \log \left[\det \left(\frac{L}{\sigma_R^2} \widetilde{\mathbf{W}} \mathbf{A} \mathbf{R}_{RC} \mathbf{A}^H \widetilde{\mathbf{W}}^H + \mathbf{I}_{N(K+N)} \right) \right] - \\ & \log \left[\det \left(\frac{L}{\sigma_R^2} \widetilde{\mathbf{W}} \mathbf{A} \mathbf{R}_C \mathbf{A}^H \widetilde{\mathbf{W}}^H + \mathbf{I}_{N(K+N)} \right) \right] \end{aligned} \quad (30a)$$

$$\text{s.t.} \quad R_k \geq r_k, \quad \forall k, \quad (30b)$$

$$\|\mathbf{W}\|_F^2 \leq P_0, \quad (30c)$$

$$|e_m|^2 = 1, \quad m = 1, \dots, M. \quad (30d)$$

Note that Problem (30) is difficult to solve because of the nonconcave objective function (30a), nonconvex constraints (30b) and coupled variables, where the sensing MI (30a) with the consideration of radar clutter interference is more complicated than that given by (13a) in Section III. Furthermore, the determinant in (30a) is challenging to tackle due to high-rank matrices \mathbf{R}_{RC} , \mathbf{R}_C and \mathbf{H}_{BI} , and the quartic term of \mathbf{E} in (30a) is also difficult to cope with. As a result, we use the MM and SDR methods to transform the nonconvex problem (30) into a convex problem approximately [42].

In order to use the MM method, we first make some transformations for the objective function (30a) denoted by $f(\mathbf{W}, \mathbf{E})$, which can be rewritten as

$$f(\mathbf{W}, \mathbf{E}) = -\log \left[\det \left(\eta (\mathbf{R}_R^{\frac{1}{2}})^H \mathbf{P}^H \widetilde{\mathbf{T}}^{-1} \mathbf{P} \mathbf{R}_R^{\frac{1}{2}} + \mathbf{I}_{M^2} \right)^{-1} \right], \quad (31a)$$

$$= -\log \left[\det \left(\mathbf{I}_{M^2} - \widetilde{\mathbf{P}}^H \mathbf{T}^{-1} \widetilde{\mathbf{P}} \right) \right], \quad (31b)$$

where $\eta = \frac{L}{\sigma_R^2}$, $\mathbf{P} = \widetilde{\mathbf{W}} \mathbf{A}$, $\widetilde{\mathbf{T}} = \mathbf{I}_{N(K+N)} + \eta \mathbf{P} \mathbf{R}_C \mathbf{P}^H$, $\mathbf{T} = \mathbf{I}_{N(K+N)} + \eta \mathbf{P} \mathbf{R}_{RC} \mathbf{P}^H$, and $\widetilde{\mathbf{P}} = \sqrt{\eta} \mathbf{P} \mathbf{R}_R^{\frac{1}{2}}$. The derivation of (31a) follows the properties of determinant $\det(\mathbf{A}^{-1}) = \frac{1}{\det(\mathbf{A})}$ and $\det(\mathbf{A}) \det(\mathbf{B}) = \det(\mathbf{A}\mathbf{B})$, and (31b) is derived from the Woodbury matrix identity [45], i.e., $(\mathbf{A} + \mathbf{UCV})^{-1} = \mathbf{A}^{-1} - \mathbf{A}^{-1} \mathbf{U} (\mathbf{C}^{-1} + \mathbf{V} \mathbf{A}^{-1} \mathbf{U})^{-1} \mathbf{V} \mathbf{A}^{-1}$.

Since \mathbf{T} is a positive definite matrix, according to Lemma 3 in [46], the equation (31b) denoted by $f(\widetilde{\mathbf{P}}, \mathbf{T})$ is jointly convex in $\{\widetilde{\mathbf{P}}, \mathbf{T}\}$. Hence, similar to the derivation of the equation (32) in [30], by using the first-order Taylor expansion, the minorizer of $f(\widetilde{\mathbf{P}}, \mathbf{T})$ at the given point $(\mathbf{P}^{(n)}, \mathbf{T}^{(n)})$ is given by

$$\eta 2 \text{Re} \left(\text{Tr}(\overline{\mathbf{A}}^{(n)} \mathbf{P}) \right) - \eta^2 \text{Tr}(\mathbf{B}^{(n)} \mathbf{P} \mathbf{R}_{RC} \mathbf{P}^H) + \text{const}_3, \quad (32)$$

where $\overline{\mathbf{A}}^{(n)} = \mathbf{R}_R^{\frac{1}{2}} (\mathbf{N}^{(n)})^{-1} (\mathbf{R}_R^{\frac{1}{2}})^H (\mathbf{P}^{(n)})^H (\mathbf{T}^{(n)})^{-1}$, $\mathbf{B}^{(n)} = (\mathbf{T}^{(n)})^{-1} \mathbf{P}^{(n)} \mathbf{R}_R^{\frac{1}{2}} (\mathbf{N}^{(n)})^{-1} (\mathbf{R}_R^{\frac{1}{2}})^H (\mathbf{P}^{(n)})^H (\mathbf{T}^{(n)})^{-1}$, $\mathbf{N}^{(n)} = \mathbf{I}_{M^2} - \eta (\mathbf{R}_R^{\frac{1}{2}})^H (\mathbf{P}^{(n)})^H (\mathbf{T}^{(n)})^{-1} \mathbf{P}^{(n)} \mathbf{R}_R^{\frac{1}{2}}$, and $\text{const}_3 = \eta \text{Tr}(\mathbf{B}^{(n)} \mathbf{T}^{(n)}) - \eta \text{Tr}(\mathbf{B}^{(n)}) - 2\eta \text{Re} \left(\text{Tr}(\overline{\mathbf{A}}^{(n)} \mathbf{P}^{(n)}) \right)$.

After applying MM method, (32) is also a nonconcave function of (\mathbf{W}, \mathbf{E}) , especially the quartic function of \mathbf{E} . Then, by utilizing some matrix transformations, we show that (32) is biconcave of $\text{vec}(\mathbf{W})$ and $\widetilde{\mathbf{E}}$ [47], and the SDR method can be used, i.e., $\widetilde{\mathbf{E}} = \widetilde{\mathbf{e}} \widetilde{\mathbf{e}}^H$ and $\widetilde{\mathbf{e}}^H = [\mathbf{e}^H, 1] \in \mathbb{C}^{M+1}$. In other words, (32) is a concave function of $\text{vec}(\mathbf{W})$ with given $\widetilde{\mathbf{E}}$ and concave function of $\widetilde{\mathbf{E}}$ with given $\text{vec}(\mathbf{W})$. This motivates us to adopt an AO algorithm to update $\text{vec}(\mathbf{W})$ and $\widetilde{\mathbf{E}}$ alternately.

A. BS Beamforming Matrix Optimization

Given $\tilde{\mathbf{E}}$, we apply the MM approach to solve the BS beamforming matrix optimization subproblem. In the following, $\mathbf{W}^{(n,l)}$ denotes the fixed point of Taylor expansion in every iteration, where the subscript n represents the n -th outer iteration of AO algorithm, and the subscript l indicates the l -th inner iteration of the MM method.

First, the first three terms in (32) can be respectively rewritten as

$$\text{Tr}(\tilde{\mathbf{A}}^{(n,l)} \mathbf{P}) = \text{vec}^H((\tilde{\mathbf{A}}^{(n,l)})^H (\mathbf{A}^{(n,l)})^H) \text{vec}(\tilde{\mathbf{W}}), \quad (33)$$

$$\text{Tr}(\mathbf{B}^{(n,l)} \mathbf{P} \mathbf{R}_{RC} \mathbf{P}^H) = \text{vec}^H(\tilde{\mathbf{W}}) \check{\mathbf{B}}^{(n,l)} \text{vec}(\tilde{\mathbf{W}}). \quad (34)$$

where $\check{\mathbf{B}}^{(n,l)} = (\mathbf{A}^{(n,l)} \mathbf{R}_{RC} (\mathbf{A}^{(n,l)})^H)^T \otimes \mathbf{B}^{(n,l)}$.

Based on (33)-(34), the equation (32) can be expressed as the function of $\text{vec}(\tilde{\mathbf{W}})$. However, in order to perform the optimization over $\text{vec}(\tilde{\mathbf{W}})$, we need to transform (32) into a concave function of $\text{vec}(\tilde{\mathbf{W}})$. The relationship between $\text{vec}(\tilde{\mathbf{W}})$ and $\text{vec}(\mathbf{W})$ is given by the following lemma.

Lemma 3 *By letting $\bar{\mathbf{w}} = \text{vec}(\mathbf{W})$, we have $\text{vec}(\tilde{\mathbf{W}}) = \Phi \bar{\mathbf{w}}^*$, where*

$$\Phi = [\mathbf{C}_1 \otimes \mathbf{I}_{\tilde{K}}, \mathbf{C}_2 \otimes \mathbf{I}_{\tilde{K}}, \dots, \mathbf{C}_{NN} \otimes \mathbf{I}_{\tilde{K}}]^T \mathbf{K}_{N\tilde{K}},$$

$\mathbf{K}_{N\tilde{K}} \in \mathbb{R}^{N\tilde{K} \times N\tilde{K}}$ is the commutation matrix, $\tilde{K} = K + N$, and $\mathbf{C}_i = \text{unvec}_{N,N}(\mathbf{c}_i) \in \mathbb{R}^{N \times N}$, $i = 1, \dots, NN$ with $\mathbf{c}_i \in \mathbb{R}^{N^2 \times 1}$ being the i -th column of the identity matrix \mathbf{I}_{N^2} .

Proof: The proof is similar to [30, Appendix B], and thus omitted here. ■

With the aid of Lemma 3 and equations (33)-(34), the minorizer (32) can be rewritten as

$$2\eta \text{Re}(\text{vec}^T((\tilde{\mathbf{A}}^{(n,l)})^H (\mathbf{A}^{(n,l)})^H) \Phi^* \bar{\mathbf{w}}) - \eta^2 \bar{\mathbf{w}}^H \tilde{\mathbf{B}} \bar{\mathbf{w}} + \text{const}_3, \quad (35)$$

where $\tilde{\mathbf{B}} = \Phi^T \left((\mathbf{A}^{(n,l)} \mathbf{R}_{RC} (\mathbf{A}^{(n,l)})^H) \otimes (\mathbf{B}^{(n,l)})^T \right) \Phi^* \succeq 0$.

Moreover, for the purpose of unifying optimization variables in the BS beamforming matrix optimization subproblem, constraints (30b) and (30c) can be respectively transformed as

$$\bar{\mathbf{w}}^H \tilde{\mathbf{h}}_k \bar{\mathbf{w}} + \Omega_k \sigma_k^2 \leq 0, \quad \forall k, \quad (36)$$

$$\bar{\mathbf{w}}^H \bar{\mathbf{w}} \leq P_0, \quad (37)$$

where $\tilde{\mathbf{h}}_k = \Omega_k \sum_{i=1, i \neq k}^K \Gamma_{k,i} + \Omega_k \tilde{\mathbf{Q}}_k - \Gamma_k$, $\Gamma_k = (\mathbf{i}_k^T \otimes \mathbf{I}_N)^H \mathbf{h}_k \mathbf{h}_k^H (\mathbf{i}_k^T \otimes \mathbf{I}_N)$, $\Gamma_{k,i} = (\mathbf{i}_i^T \otimes \mathbf{I}_N)^H \mathbf{h}_k \mathbf{h}_k^H (\mathbf{i}_i^T \otimes \mathbf{I}_N)$, $\tilde{\mathbf{Q}}_k = (\mathbf{Q}^* \mathbf{Q}^T \otimes \mathbf{h}_k \mathbf{h}_k^H)$, $\mathbf{h}_k^H = \mathbf{h}_{\text{BU},k}^H + \mathbf{h}_{\text{IU},k}^H \mathbf{E} \mathbf{H}_{\text{BI}}$, $\mathbf{Q}^T = [\mathbf{0}_{N \times K}, \mathbf{I}_N]$, and \mathbf{i}_k is the k -th column of the identity matrix \mathbf{I}_{K+N} .

Note that communication rate constraints (36) are nonconvex, and successive convex approximation (SCA) method is applied to transform them into convex constraints, which are given by

$$\begin{aligned} & -2\text{Re}((\bar{\mathbf{w}}^{(n,l)})^H \Gamma_k \bar{\mathbf{w}}) + (\bar{\mathbf{w}}^{(n,l)})^H \Gamma_k \bar{\mathbf{w}}^{(n,l)} \\ & + \Omega_k \left(\sum_{i=1, i \neq k}^K \bar{\mathbf{w}}^H \Gamma_{k,i} \bar{\mathbf{w}} + \sigma_k^2 + \bar{\mathbf{w}}^H \tilde{\mathbf{Q}}_k \bar{\mathbf{w}} \right) \leq 0, \quad \forall k. \end{aligned} \quad (38)$$

After discarding the constant in (35), dividing (35) by η , substituting (30b) with (38), replacing (30c) by (37), and transforming the maximization problem into minimization problem, the optimization subproblem of Problem (30) corresponding to BS beamforming matrix can be reformulated as

$$\min_{\bar{\mathbf{w}}} \quad -2\text{Re}(\bar{\mathbf{w}}^H \Phi^T \text{vec}^*((\tilde{\mathbf{A}}^{(n,l)})^H (\mathbf{A}^{(n,l)})^H)) + \eta \bar{\mathbf{w}}^H \tilde{\mathbf{B}} \bar{\mathbf{w}} \quad (39a)$$

$$\text{s.t.} \quad (37), (38). \quad (39b)$$

As a result, Problem (39) becomes an SOCP problem which can be solved using CVX.

B. IRS Reflection Coefficients Optimization

When BS beamforming matrix \mathbf{W} is fixed, we need to transform Problem (30) into a convex problem of $\tilde{\mathbf{E}}$. As aforementioned, SDR method is applied to deal with the quartic term of \mathbf{E} in the minorizer (32). In order to facilitate this transformation, the following equality is used [45],

$$\text{Tr}(\text{diag}(\mathbf{a})^H \mathbf{B} \text{diag}(\mathbf{c}) \mathbf{D}^T) = \mathbf{a}^H (\mathbf{B} \circ \mathbf{D}) \mathbf{c}. \quad (40)$$

By using (40), the other terms except the constant in the minorizer (32) can be respectively rewritten as

$$\text{Tr}(\tilde{\mathbf{A}}^{(n)} \mathbf{P}) = \mathbf{1}_{N(K+N)}^H (\mathbf{V}^{(n)} \circ (\tilde{\mathbf{A}}^{(n)})^T) \mathbf{j}, \quad (41)$$

$$\text{Tr}(\mathbf{B}^{(n)} \mathbf{P} \mathbf{R}_{RC} \mathbf{P}^H) = \mathbf{j}^H ((\mathbf{V}^{(n)})^H \mathbf{B}^{(n)} \mathbf{V}^{(n)} \circ \mathbf{R}_{RC}^T) \mathbf{j}. \quad (42)$$

where $\mathbf{J} = \mathbf{E}^T \otimes \mathbf{E}^H$, $\mathbf{V}^{(n)} = \tilde{\mathbf{W}}^{(n)} (\mathbf{H}_{\text{BI}}^T \otimes \mathbf{H}_{\text{BI}}^H)$, and \mathbf{j} is the column vector comprised of the diagonal elements of \mathbf{J} , i.e., $\mathbf{j} = \text{vec}([\tilde{\mathbf{E}}]_{1:M,1:M})$.

Hence, given \mathbf{W} , maximizing (32) is equivalent to minimizing the following expression,

$$\eta \mathbf{j}^H \bar{\mathbf{V}}^{(n)} \mathbf{j} - 2\text{Re}(\mathbf{1}_{N(K+N)}^H (\mathbf{V}^{(n)} \circ (\tilde{\mathbf{A}}^{(n)})^T) \mathbf{j}), \quad (43)$$

where $\bar{\mathbf{V}}^{(n)} = ((\mathbf{V}^{(n)})^H \mathbf{B}^{(n)} \mathbf{V}^{(n)} \circ \mathbf{R}_{RC}^T) \succeq 0$. Here, similar to (39a), we discard the constant in (32) and divide the remaining terms by a coefficient η .

Then, with the use of SDR, communication rate constraints (30b) can be transformed into

$$\begin{aligned} & \Omega_k \left(\sum_{i=1, i \neq k}^K \text{Tr}(\tilde{\mathbf{E}} \mathbf{H}_k \mathbf{w}_i \mathbf{w}_i^H \mathbf{H}_k^H) + \text{Tr}(\tilde{\mathbf{E}} \mathbf{H}_k \mathbf{W}_R \mathbf{W}_R^H \mathbf{H}_k^H) \right. \\ & \left. + \sigma_k^2 \right) - \text{Tr}(\tilde{\mathbf{E}} \mathbf{H}_k \mathbf{w}_k \mathbf{w}_k^H \mathbf{H}_k^H) \leq 0, \quad \forall k, \end{aligned} \quad (44)$$

where $\mathbf{H}_k = [\mathbf{H}_{\text{BI}}^H \text{diag}(\mathbf{h}_{\text{IU},k}^H)^H, \mathbf{h}_{\text{BU},k}]^H$ represents the equivalent channel from the BS to the k -th user.

Therefore, replacing (30b) with (44), transforming maximization problem into minimization problem and dismissing the rank-one constraint, the optimization subproblem of Problem (30) corresponding to IRS reflection coefficients matrix \mathbf{E} is recast as

$$\min_{\tilde{\mathbf{E}}} \quad (43) \quad (45a)$$

$$\text{s.t.} \quad (44),$$

$$[\text{Diag}(\tilde{\mathbf{E}})]_m = 1, \quad m = 1, \dots, M+1, \quad (45b)$$

$$\tilde{\mathbf{E}} \succeq 0. \quad (45c)$$

Problem (45) is a standard SDP problem which can be solved using CVX. Upon obtaining the optimal solution to Problem (45) without rank-1 constraint, Gaussian randomization method can be adopted to construct a suboptimal rank-1 solution [41]. More specifically, denoting $\hat{\mathbf{E}}_1$ as the rank-relaxed solution to Problem (45), its EVD is given by $\hat{\mathbf{E}}_1 = \mathbf{U}_1 \mathbf{\Sigma}_1 \mathbf{U}_1^H$, where $\mathbf{\Sigma}_1$ is the diagonal matrix with diagonal elements being the eigenvalues of $\hat{\mathbf{E}}_1$, and every column in \mathbf{U}_1 is an eigenvector of $\hat{\mathbf{E}}_1$. Next, 1000 random candidate vectors are generated as $\hat{\mathbf{e}}_i = \exp\left(j\angle\left(\frac{\mathbf{U}_1 \mathbf{\Sigma}_1^{\frac{1}{2}} \mathbf{q}_i}{[\mathbf{U}_1 \mathbf{\Sigma}_1^{\frac{1}{2}} \mathbf{q}_i]_{M+1}}\right)\right)$, $i = 1, \dots, 1000$, where \mathbf{q}_i follows complex Gaussian distribution with zero mean and unit variance, i.e., $\mathbf{q}_i \sim \mathcal{CN}(0, \mathbf{I}_{M+1})$. Based on this, the suboptimal rank-1 solution to Problem (45) is selected from $\hat{\mathbf{E}} = [\text{diag}(\hat{\mathbf{e}}_i^*)]_{1:M, 1:M}$ satisfying all constraints in Problem (30) and maximizing the sensing MI (30a). Furthermore, a sufficiently large times of Gaussian randomization are necessary to ensure the non-decreasing objective function (30a).

In the end, the overall algorithm to solve Problem (30) is outlined in Algorithm 2.

Algorithm 2 Generalized Iterative Algorithm for Solving Problem (30)

- 1: Set the outer iteration index $n = 0$. Initialize $\mathbf{E}^{(0)}$, $\mathbf{W}^{(0)}$, the tolerance ϵ_2 , and the maximum iterations number \mathcal{Q}_{max} .
 - 2: **repeat**
 - 3: Given $\mathbf{E}^{(n)}$, let the inner iteration index $l = 0$ and $\mathbf{W}^{(n,l)} = \mathbf{W}^{(n)}$.
 - 4: **repeat**
 - 5: Obtain $\mathbf{W}^{(n,l+1)}$ by solving Problem (39), and then $l = l + 1$.
 - 6: **until** convergence or reaching the maximum iterations number.
 - 7: Let $\mathbf{W}^{(n+1)} = \mathbf{W}^{(n,l)}$.
 - 8: Given $\mathbf{W}^{(n+1)}$, obtain the IRS reflection coefficients matrix without rank-1 constraint by solving Problem (45). Then, the rank-1 solution $\mathbf{E}^{(n+1)}$ can be constructed by the Gaussian randomization method.
 - 9: Set $n = n + 1$.
 - 10: **until** the fractional increase of objective function value (30a) is less than ϵ_2 or the iteration number is more than \mathcal{Q}_{max} .
-

C. Initialization

Algorithm 2 needs to be initialized by a feasible point, which can greatly affect the performance of the converged suboptimal solution. The initial point can be obtained by guaranteeing the QoS of the communication task without considering the sensing task. First, the IRS reflection coefficients can be optimized by maximizing the weighted channel gain [10], i.e., $\arg \max_{\mathbf{E} \in \{|e_m|^2=1, \forall m\}} \sum_{k=1}^K \omega_k \|(\mathbf{h}_{\text{BU},k}^H + \mathbf{h}_{\text{IU},k}^H \mathbf{E} \mathbf{H}_{\text{BI}})\|^2$, where $\omega_k = \frac{1}{\Omega_k \sigma_k^2}$. This optimization problem can be solved

by SDR and Gaussian randomization method, and the details, which are shown in [10], are omitted here. Second, given \mathbf{E} , we just need to find a feasible BS beamforming matrix \mathbf{W} to Problem (30), where the feasible solution can be obtained by adopting SDR method and Theorem 1.

D. Convergence Analysis

In this subsection, we analyze the convergence of Algorithm 2. Let the objective function (30a) and the minorizer (32) be denoted by $f(\mathbf{W}, \mathbf{E})$ and $g(\mathbf{W}^{(n,l)} | \mathbf{W}^{(n)}, \mathbf{E}^{(n)})$, respectively. Hence, in the inner iteration from Steps 4 to 6, given $\mathbf{E}^{(n)}$, we have

$$\begin{aligned} f(\mathbf{W}^{(n)}, \mathbf{E}^{(n)}) &\stackrel{(a)}{=} g(\mathbf{W}^{(n,l)} | \mathbf{W}^{(n)}, \mathbf{E}^{(n)}) \\ &\stackrel{(b)}{\leq} g(\mathbf{W}^{(n,l+1)} | \mathbf{W}^{(n)}, \mathbf{E}^{(n)}) \stackrel{(c)}{\leq} f(\mathbf{W}^{(n+1)}, \mathbf{E}^{(n)}), \end{aligned} \quad (46)$$

where $\mathbf{W}^{(n)} = \mathbf{W}^{(n,l)}$, $\mathbf{W}^{(n+1)} = \mathbf{W}^{(n,l+1)}$, (a) follows the MM condition (A1) in [11], (b) is due to the optimality of maximization problem (39), and (c) follows the MM condition (A2) in [11]. Furthermore, the non-decreasing minorizer (32) has a finite upper bound because of the bounded feasible set. Therefore, the objective function (30a) in the inner iteration can converge to a finite value.

Then, given $\mathbf{W}^{(n+1)}$, similarly to (46), the following relationship holds:

$$\begin{aligned} f(\mathbf{E}^{(n)}, \mathbf{W}^{(n+1)}) &= g(\mathbf{E}^{(n)} | \mathbf{E}^{(n)}, \mathbf{W}^{(n+1)}) \\ &\leq g(\mathbf{E}^{(n+1)} | \mathbf{E}^{(n)}, \mathbf{W}^{(n+1)}) \leq f(\mathbf{E}^{(n+1)}, \mathbf{W}^{(n+1)}). \end{aligned} \quad (47)$$

Due to the bounded feasible set, the non-decreasing objective function (30a) has a finite upper bound, which prove that the convergence of the sequence $f(\mathbf{E}^{(n)}, \mathbf{W}^{(n)})$ in Algorithm 2.

E. Complexity Analysis

The major complexity of Algorithm 2 in every outer iteration lies in solving SOCP problem (39) by MM framework and SDP problem (45). Similar to the complexity analysis of Algorithm 1, the approximate complexity of Problem (39) is $\mathcal{O}(N(K+N)(K+1)^{3.5} + N(K+N)(K+1)^{2.5})$, and that of Problem (45) is given by $\mathcal{O}([(K+1)(M+1)]^{\frac{1}{2}} M[M^2 + M(K+1)(M+1)^2 + (K+1)(M+1)^3])$. Hence, the total complexity of Algorithm 2 per outer iteration is approximately given by $\mathcal{O}(l_2[N(K+N)(K+1)^{3.5} + N(K+N)(K+1)^{2.5}] + [(K+1)(M+1)]^{\frac{1}{2}} M[M^2 + M(K+1)(M+1)^2 + (K+1)(M+1)^3])$, where l_2 denotes the inner iteration number from Steps 4 to 6.

V. NUMERICAL RESULTS

In this section, numerical results are provided to evaluate the performance of our proposed algorithms in the IRS-aided MIMO ISAC system. Both the BS and the IRS employ ULA with $N = 8$ antennas and $M = 32$ reflecting elements, respectively. The Cartesian coordinate system is adopted in our paper, where the BS is located at (0 m, 0 m), the IRS is located at (50 m, 10 m), and communication users are randomly distributed in the circle centered at (60 m, 0 m) with the radius of 2.5 m. The channels from the BS to the k -th user, $\mathbf{h}_{\text{BU},k}$, and from the IRS to the k -th user, $\mathbf{h}_{\text{IU},k}$, are assumed to be Rician fading with Rician factor 0.5. Meanwhile, the channel between the BS and the IRS, \mathbf{H}_{BI} , is considered in

two cases: LoS only as the product of the steering vector of transceivers and Rician fading with Rician factor 0.5. The transmit/receive steering vector of the BS or the IRS is given by $\mathbf{a}(\theta) = \mathbf{b}(\theta) = [1, e^{-i\frac{2\pi d_1}{\lambda_1} \sin \theta}, \dots, e^{-i\frac{2\pi(N_1-1)d_1}{\lambda_1} \sin \theta}]$, where λ_1 is the wavelength, N_1 is the number of antennas or reflecting elements, and $d_1 = \frac{\lambda_1}{2}$ is the antenna or reflecting element spacing. Next, the large-scale path loss coefficient is $-30 - 10\alpha \log_{10}(d)$ dB, in which d is the link length in meters and the path loss exponents α for the BS-IRS link, the IRS-users link and the BS-users link are respectively set as 2.5, 2.5, and 3.5. We consider two types of the sensing targets: the point target, i.e., $N_r = 1$, located at the angle $\theta^r = 0^\circ$ with the average strength $\beta^2 = -20$ dB and the extended target, i.e., $N_r = 3$, with directions $\theta_1^r = -30^\circ, \theta_2^r = 0^\circ$ and $\theta_3^r = 30^\circ$ and average strength $\beta_1^2 = \beta_2^2 = \beta_3^2 = -20$ dB [35]. Furthermore, the clutter interference is located at $\theta_1^c = -80^\circ, \theta_2^c = -50^\circ, \theta_3^c = -10^\circ, \theta_4^c = 10^\circ, \theta_5^c = 50^\circ, \theta_6^c = 80^\circ$, i.e., $N_c = 6$, with the average strength $\gamma_q^c = 0$ dB, $q = 1, \dots, N_c$ [48], [49]. The number of communication users are set as $K = 3$ with the required communication rate threshold $r_k = 3$ bps/Hz, $k = 1, \dots, K$. In addition, the power budget of the BS is $P_0 = 40$ dBm, the noise power is $\sigma_R^2 = \sigma_k^2 = -80$ dBm, $k = 1, \dots, K$, and the length of communication time slots, which is also the number of radar fast-time snapshots, is set to $L = 64$. As for the stopping criteria in Algorithms 1 and 2, we set $\epsilon_o = 10^{-7}$, $\epsilon_i = \epsilon_2 = 10^{-5}$ and $\epsilon_d = 10^{-3}$.

Our proposed schemes in Sections III and IV are denoted by Algorithm 1 and Algorithm 2, respectively. To further evaluate the performance of our proposed algorithms, the following benchmarks are used for comparison.

1) BP: This is the scheme in Algorithm 2 of [25], based on the beampattern (BP) metric.

2) SNR: This is the scheme in [19], where the sensing SNR metric is applied to design IRS-aided MIMO ISAC beamforming scheme.

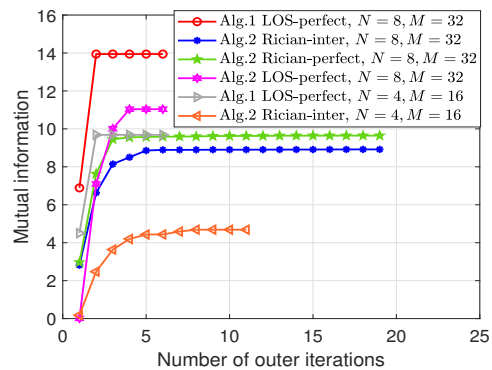
3) CBO: This approach optimizes the communication beamforming matrix only (CBO) with $\mathbf{W}_R = 0$ in our proposed algorithms.

4) SO: In this scheme, IRS reflection coefficients and BS beamformer are optimized separately, i.e., separate optimization (SO). We firstly obtain \mathbf{E} by maximizing the weighted sum of the norms of the IRS cascaded channels in the desired sensing directions, i.e., $\max_{\mathbf{E}} \sum_{p=1}^{N_r} \|\mathbf{b}(\theta_p^r)^H \mathbf{E} \mathbf{H}_{\text{BI}}\|^2$. Next, \mathbf{W} is optimized by solving Problem (39).

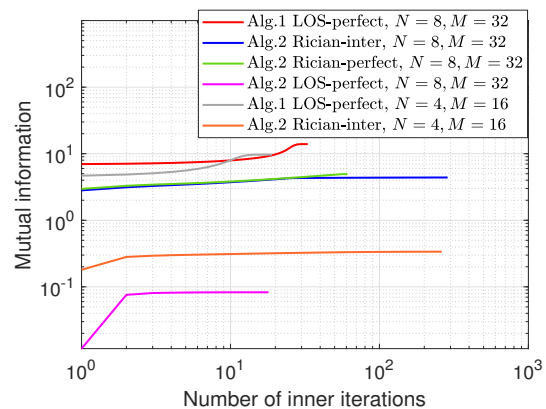
5) Random: In this scenario, IRS reflection coefficients are generated randomly within the range of $[0, 2\pi)$. Then, the BS beamforming matrix can be obtained by solving Problem (39).

A. Convergence Performance and Computational Time

In this subsection, we exhibit the convergence performance and the computational time of our proposed algorithms and consider the point sensing target. When there is no clutter interference, i.e., $\mathbf{R}_C = 0$, we denote Algorithm 1 with \mathbf{H}_{BI} being LoS channel, Algorithm 2 considering LoS channel for \mathbf{H}_{BI} and Algorithm 2 with \mathbf{H}_{BI} being Rician channel as "Alg.1 LOS-perfect", "Alg.2 LOS-perfect" and "Alg.2 Rician-perfect", respectively.



(a) Achievable MI versus the number of outer iterations.



(b) Achievable MI versus the number of inner iterations.

Fig. 2: Achievable MI versus the number of algorithm iterations.

Then, let "Alg.2 Rician-inter" represent the situation where no clutter interference is present, and \mathbf{H}_{BI} is Rician channel.

Fig. 2 illustrates the convergence performance of our proposed Algorithms 1 and 2. From Fig. 2, we can observe that "Alg.1 LOS-perfect" can converge to a better suboptimal point with 6 outer iterations and dozens of inner iterations than "Alg.2 LOS-perfect". This result shows that although Algorithm 2 can also be applied to the simplified case, Algorithm 1 is more suitable for the situation where the clutter interference does not exist, and \mathbf{H}_{BI} is LoS channel. When \mathbf{H}_{BI} is Rician channel, "Alg.2 Rician-perfect" can achieve higher MI than "Alg.2 Rician-inter" with the same number of outer iterations and less inner iterations. In addition, from the comparison between the case of $N = 4, M = 16$ and the case of $N = 8, M = 32$, it is revealed that the increased numbers of BS antennas and IRS reflecting elements can improve the MI.

Fig. 3 shows the computational time of our proposed algorithms versus the number of outer iterations. The total computational time that "Alg.1 LOS-perfect" needs to converge is about 35 s, which is 100 s faster than "Alg.2 LOS-perfect". This further depicts the low-complexity of Algorithm 1 compared to Algorithm 2 in the simplified case. Nevertheless, the advantage of Algorithm 2 is that it can be applied to the generalized case, where "Alg.2 Rician-inter" takes approximately 824 s to converge, which is almost the same as

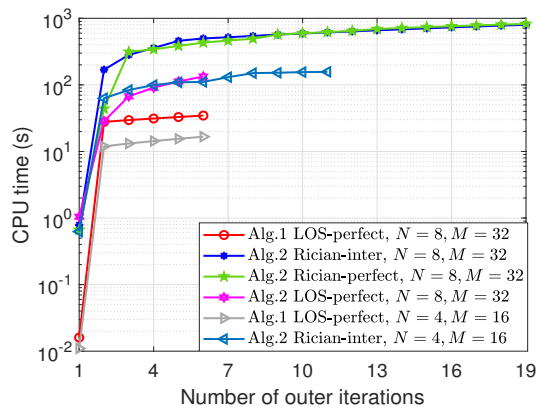


Fig. 3: The computational time of the proposed algorithms versus the number of outer iterations.

"Alg.2 Rician-perfect". This shows that the existence of the clutter interference doesn't cause a large fluctuation in the total time for Algorithm 2.

B. IRS-aided ISAC Beamforming Design in Simplified Case

In this subsection, we investigate the performance of the situation where clutter interference is not present, and LoS channel is considered for \mathbf{H}_{BI} . Unless otherwise specified, the point sensing target is considered.

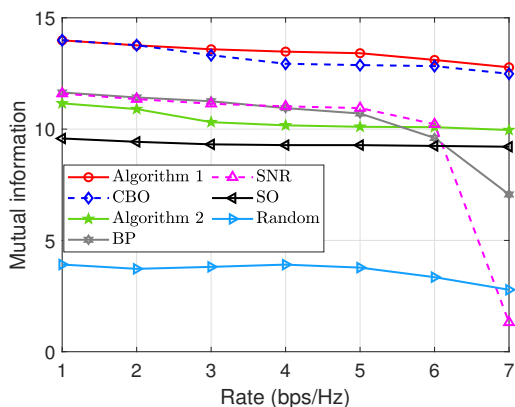


Fig. 4: Achievable MI versus the communication rate requirement.

Fig. 4 plots the achievable MI versus the communication rate requirement. As proved in Lemma 1, the sensing MI of Algorithm 1 is equal to that of CBO when $r \leq 2$ bps/Hz, and is higher than the sensing MI of CBO when $3 \leq r \leq 7$ bps/Hz. This is because, at low communication rates, most of the BS's beams are directed towards the reflected link created by the IRS, effectively weakening the direct link. However, at high communication rates, the communication demand cannot be met solely through the reflected link created by the IRS, hence more beams are pointed to the direct link. It is shown in Fig. 4 that, Algorithm 1 can obtain better sensing performance than the other benchmarks. With the increase of the communication rate requirement, the value of MI of all of schemes gradually decreases. This is due to the tradeoff between the sensing and communication performance

in the IRS-aided ISAC system, i.e., the increasing demand of communication can bring negative impacts on the sensing performance. However, when $r = 6$ bps/Hz, the achievable MI of BP-based and SNR-based schemes degrade sharply while the achievable MI of other schemes have a steady decline. This reveals the performance superiority of our proposed algorithms in the situation where communication QoS is high. In addition, Random has the worst performance on MI, which shows that the MI in our considered case with IRS working as a colocated MIMO radar is greatly affected by IRS reflecting coefficients. This is contrary to the results in the case of IRS working as the statistical MIMO radar [32].

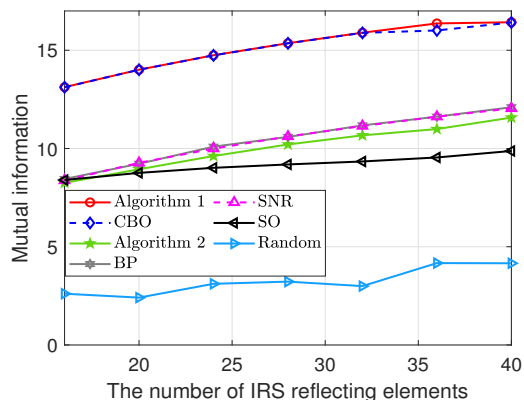


Fig. 5: Achievable MI versus the number of IRS reflecting elements.

Fig. 5 shows the achievable MI versus the number of IRS reflecting elements. First, with the increase of the number of IRS reflecting elements, the value of MI for all schemes except Random has a growing trend, which exhibits more MI gain from more IRS reflecting elements and signifies again the effects of IRS reflecting coefficients on the sensing performance. Second, similar to Fig. 4, Algorithm 1 achieves the best MI, but the sensing MI of CBO is almost the same as that of Algorithm 1, which verifies Lemma 1 and shows the performance superiority of Algorithm 1 again.

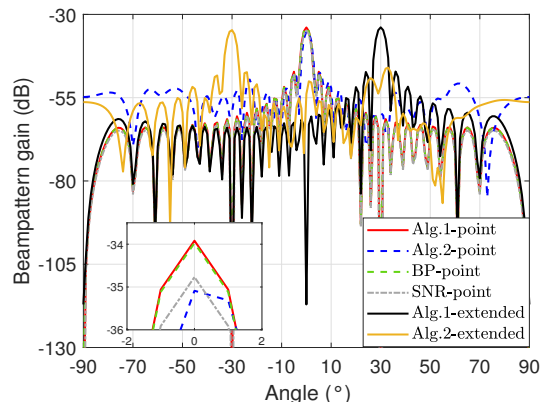


Fig. 6: Beampatterns without clutter interference in the scenario of LoS channel for \mathbf{H}_{BI} .

Fig. 6 illustrates the beampatterns of different schemes in the simplified case with no clutter interference and \mathbf{H}_{BI} being

LoS channel. "Alg.1-extended" and "Alg.2-extended" respectively represent the cases when the problem with an extended target is solved by Algorithm 1 and Algorithm 2. In the scenario of the point target, the beampattern of "Alg.1-point" is almost the same as that of "BP-point" and has the highest mainlobe directed to the target angle 0° with about 1dB higher than the SNR-based and Algorithm 2-based schemes. This demonstrates that the proposed Algorithm 1 has the best sensing performance compared to other benchmarks. However, from "Alg.1-extended" and "Alg.2-extended", we can observe that the extended target cannot be sensed thoroughly, and the beampatterns can only point to one direction with the other two sensing directions unperceived. This is because the rank-1 LoS channel \mathbf{H}_{BI} can only distinguish one sensing parameter.

C. IRS-aided ISAC Beamforming Design in Generalized Case

In this subsection, we consider the extended sensing target and Rician channel for \mathbf{H}_{BI} .

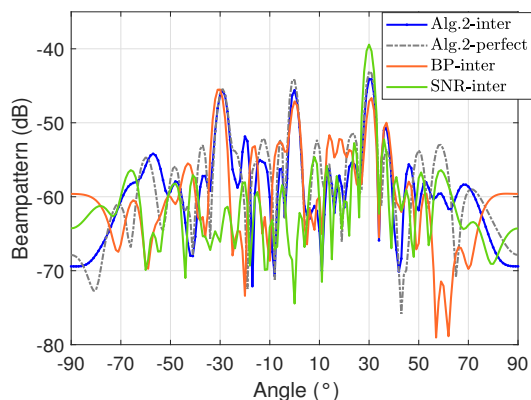


Fig. 7: Beampatterns with clutter interference in the scenario of Rician channel for \mathbf{H}_{BI} .

Fig. 7 compares the beampatterns of different algorithms. The beamforming problem without clutter interference solved by Algorithm 2 is denoted as "Alg.2-perfect", and the other schemes with clutter interference are respectively denoted as "Alg.2-inter", "BP-inter" and "SNR-inter". First, compared to "Alg.1-extended" in Fig. 6, the beampatterns of "Alg.2-perfect" and "Alg.2-inter" can identify all directions of the extended target, which shows that Rician channel with high rank can provide more gain for parameter sensing compared with the LoS channel. Second, in presence of clutter interference, the beampattern of "SNR-inter" only has one mainlobe directed to the angle 30° while the other desired sensing angles are missed. By contrast, our proposed scheme based on Algorithm 2 can perceive every sensing direction and has better beampattern than "SNR-inter" and "BP-inter". Third, from the comparison between "Alg.2-inter" and "Alg.2-perfect", the mainlobe of "Alg.2-inter" is lower than that of "Alg.2-perfect", and the sidelobes of "Alg.2-inter" in some angles of clutter interference, e.g., 10° , 50° and 80° , are suppressed effectively. This illustrates that our proposed Algorithm 2 can achieve good beampattern while suppressing the clutter interference effectively.

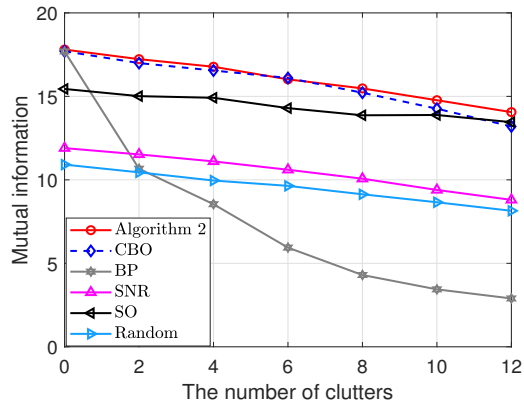


Fig. 8: Achievable MI versus the number of clutters.

Fig. 8 depicts the achievable MI versus the number of clutters N_c . All considered schemes have the highest value of MI when $N_c = 0$, i.e., there is no clutter interference, and their achievable MI gradually degrades with the increase of the number of clutters, especially for BP which has a sharp decline of MI. This shows that more interfering scatterers can cause higher performance loss on MI. Besides, the MI of Algorithm 2 is slightly higher than that of CBO but outperforms the other benchmarks significantly, which reveals that the improvement of MI due to dedicated sensing beamforming is limited, and our proposed Algorithm 2 is more robust to the clutter interference than the other schemes.

VI. CONCLUSIONS

In this paper, we studied an IRS-aided MIMO ISAC system based on sensing MI, by utilizing IRS as a colocated MIMO radar. We considered two cases: the simplified case with LoS BS-IRS channel and no clutter interference to sensing, and the generalized case with Rician fading channel for the BS-IRS link and the presence of clutter interference to sensing. For both cases, we formulated the optimization problem by maximizing the sensing MI, subject to the QoS constraints for all communication users, the transmit power constraint at the BS, and the unit-modulus constraint on the IRS's passive reflection. In the first case, we showed that the dedicated sensing beamformer cannot improve the sensing performance if the direct links between the BS and communication users are completely blocked, and proposed a low-complexity iterative algorithm for solving the formulated optimization problem. In the second case, an alternative iterative algorithm, which can also be applied to the first case, was provided to solve the problem under the general setup. Numerical results were presented to demonstrate the performance superiority of proposed algorithms in comparison to various benchmark schemes.

APPENDIX A THE PROOF OF LEMMA 1

First, the communication-only beamforming problem without dedicated sensing beamformer is formulated as

$$\max_{\mathbf{C}_X, \mathbf{W}_1, \dots, \mathbf{W}_K} \quad (18a) \quad (48a)$$

s.t. (18b), (18c), (48b)

$$\mathbf{C}_X = \sum_{k=1}^K \mathbf{W}_k, \quad \mathbf{W}_k \succeq 0, \quad \forall k. \quad (48c)$$

Next, we prove that the optimal value of Problem (18) can be always achieved by a communication-only beamforming matrix satisfying the constraints of Problem (48).

Assuming that the optimal rank-1 solution to Problem (18) is $\hat{\mathbf{C}}_X$ and $\hat{\mathbf{W}}_k, k = 1, \dots, K$, we can construct a communication-only beamforming matrix as $\check{\mathbf{W}}_k = \hat{\mathbf{W}}_k + \iota_k \hat{\mathbf{C}}_R$ with $\hat{\mathbf{C}}_R = \hat{\mathbf{C}}_X - \sum_{k=1}^K \hat{\mathbf{W}}_k$ and $\sum_{k=1}^K \iota_k = 1, \iota_k \geq 0$. Then, we can verify that $\check{\mathbf{W}}_k$ is also feasible to Problem (48), i.e., constraints (18b) and (18c) are respectively given by

$$\begin{aligned} & \Omega_k \text{Tr}(\mathbf{h}_k \mathbf{h}_k^H \sum_{k=1}^K \check{\mathbf{W}}_k) - (1 + \Omega_k) \text{Tr}(\mathbf{h}_k \mathbf{h}_k^H \check{\mathbf{W}}_k) + \Omega_k \sigma_k^2 \\ &= \Omega_k \text{Tr}(\mathbf{h}_k \mathbf{h}_k^H (\sum_{k=1}^K \hat{\mathbf{W}}_k + \hat{\mathbf{C}}_R)) + \Omega_k \sigma_k^2 \\ & \quad - (1 + \Omega_k) \text{Tr}(\mathbf{h}_k \mathbf{h}_k^H (\hat{\mathbf{W}}_k + \iota_k \hat{\mathbf{C}}_R)) \\ & \leq \Omega_k \text{Tr}(\mathbf{h}_k \mathbf{h}_k^H (\sum_{k=1}^K \hat{\mathbf{W}}_k + \hat{\mathbf{C}}_R)) - (1 + \Omega_k) \text{Tr}(\mathbf{h}_k \mathbf{h}_k^H \hat{\mathbf{W}}_k) \\ & \quad + \Omega_k \sigma_k^2 \leq 0, \quad \forall k, \end{aligned} \quad (49)$$

$$\text{Tr}(\sum_{k=1}^K \check{\mathbf{W}}_k) = \text{Tr}(\sum_{k=1}^K \hat{\mathbf{W}}_k + \hat{\mathbf{C}}_R) \leq P_0, \quad (50)$$

where the first equality in (49) follows from $\sum_{k=1}^K \iota_k = 1$, the first inequality in (49) follows from $\hat{\mathbf{C}}_R \succeq 0$ and $\iota_k(1 + \Omega_k) \text{Tr}(\mathbf{h}_k \mathbf{h}_k^H \hat{\mathbf{C}}_R) \geq 0$, and the second inequality in (49) and the first inequality in (50) follow from the optimality of $\hat{\mathbf{C}}_X$ and $\hat{\mathbf{W}}_k, k = 1, \dots, K$.

Furthermore, the objective function (48a) can be written as

$$\mathbf{a}^H(\theta_B) \sum_{k=1}^K \check{\mathbf{W}}_k \mathbf{a}(\theta_B) = \mathbf{a}^H(\theta_B) (\sum_{k=1}^K \hat{\mathbf{W}}_k + \hat{\mathbf{C}}_R) \mathbf{a}(\theta_B). \quad (51)$$

Note that Problem (48) with the feasible solution $\check{\mathbf{W}}_k, k = 1, \dots, K$, has the same value of the objective function as Problem (18) with the optimal solution $\hat{\mathbf{C}}_X$ and $\hat{\mathbf{W}}_k, k = 1, \dots, K$. Then, due to the fact that the feasible set of Problem (48) is a subset of the feasible set of Problem (18), $\check{\mathbf{W}}_k, k = 1, \dots, K$, is the optimal solution to Problem (48). Thus, the optimality of Problem (18) can be achieved by the optimal solution to Problem (48) with $\mathbf{W}_R = \mathbf{0}$.

Although removing the dedicated sensing beamforming matrix \mathbf{W}_R does not affect the optimality of Problem (18), the reconstructed rank-1 solution by Gaussian randomization to Problem (48) causes performance loss on the sensing MI inevitably. Hence, we prove that when $\mathbf{h}_{\text{BU},k} = 0$, by using Theorem 1, there exists a rank-1 optimal solution $\check{\mathbf{W}}_k$ for Problem (48), which achieves the optimality of Problem (18).

In the communication-only beamforming problem, we can also construct the rank-1 solution based on Theorem 1, i.e.,

$$\bar{\mathbf{w}}_k = (\mathbf{h}_k^H \check{\mathbf{W}}_k \mathbf{h}_k)^{-\frac{1}{2}} \check{\mathbf{W}}_k \mathbf{h}_k, \quad \bar{\mathbf{W}}_k = \bar{\mathbf{w}}_k \bar{\mathbf{w}}_k^H. \quad (52)$$

For the SINR constraints (18b), we have

$$\begin{aligned} & \Omega_k \text{Tr}(\mathbf{h}_k \mathbf{h}_k^H \sum_{k=1}^K \bar{\mathbf{W}}_k) - (1 + \Omega_k) \text{Tr}(\mathbf{h}_k \mathbf{h}_k^H \bar{\mathbf{W}}_k) + \Omega_k \sigma_k^2 \\ &= \Omega_k \text{Tr}(\mathbf{h}_k \mathbf{h}_k^H \sum_{k=1}^K \check{\mathbf{W}}_k) - (1 + \Omega_k) \text{Tr}(\mathbf{h}_k \mathbf{h}_k^H \check{\mathbf{W}}_k) + \Omega_k \sigma_k^2 \\ & \leq 0, \quad \forall k. \end{aligned} \quad (53)$$

For the power constraint (18c), we can prove the following equalities/inequalities:

$$\begin{aligned} \text{Tr}(\sum_{k=1}^K \bar{\mathbf{W}}_k) &= \sum_{k=1}^K (\mathbf{h}_k^H \check{\mathbf{W}}_k \mathbf{h}_k)^{-1} \text{Tr}(\check{\mathbf{W}}_k \mathbf{h}_k \mathbf{h}_k^H \check{\mathbf{W}}_k^H) \\ &= \sum_{k=1}^K (\mathbf{h}_k^H \check{\mathbf{W}}_k \mathbf{h}_k)^{-1} \mathbf{h}_k^H (\check{\mathbf{W}}_k^{\frac{1}{2}})^H \check{\mathbf{W}}_k \check{\mathbf{W}}_k^{\frac{1}{2}} \mathbf{h}_k \\ &= \sum_{k=1}^K (\mathbf{h}_k^H \check{\mathbf{W}}_k \mathbf{h}_k)^{-1} \mathbf{h}_k^H (\check{\mathbf{W}}_k^{\frac{1}{2}})^H \mathbf{V}_k \mathbf{\Lambda}_k \mathbf{V}_k^H \check{\mathbf{W}}_k^{\frac{1}{2}} \mathbf{h}_k \\ & \leq \sum_{k=1}^K \nu_k (\mathbf{h}_k^H \check{\mathbf{W}}_k \mathbf{h}_k)^{-1} \mathbf{h}_k^H (\check{\mathbf{W}}_k^{\frac{1}{2}})^H \check{\mathbf{W}}_k^{\frac{1}{2}} \mathbf{h}_k \\ & \leq \sum_{k=1}^K \nu_k \leq \text{Tr}(\sum_{k=1}^K \check{\mathbf{W}}_k) \leq P_0, \end{aligned} \quad (54)$$

where the EVD of $\check{\mathbf{W}}_k$ is given by $\check{\mathbf{W}}_k = \mathbf{V}_k \mathbf{\Lambda}_k \mathbf{V}_k^H$, which follows from the fact that $\check{\mathbf{W}}_k$ is a Hermitian matrix, $\nu_k = \lambda_{\max}(\check{\mathbf{W}}_k)$, and the third inequality follows from the property of the positive semidefinite matrix.

As for the objective function, we have

$$\begin{aligned} & \mathbf{a}^H(\theta_B) \sum_{k=1}^K \bar{\mathbf{W}}_k \mathbf{a}(\theta_B) \\ &= \sum_{k=1}^K (\mathbf{h}_k^H \check{\mathbf{W}}_k \mathbf{h}_k)^{-1} \mathbf{h}_k^H \check{\mathbf{W}}_k^H \mathbf{A}(\theta_B) \check{\mathbf{W}}_k \mathbf{h}_k \\ &= \sum_{k=1}^K (\mathbf{h}_k^H \check{\mathbf{W}}_k \mathbf{h}_k)^{-1} \mathbf{h}_k^H (\check{\mathbf{W}}_k^{\frac{1}{2}})^H \tilde{\mathbf{A}}_k \check{\mathbf{W}}_k^{\frac{1}{2}} \mathbf{h}_k \\ & \leq \sum_{k=1}^K \varpi_k (\mathbf{h}_k^H \check{\mathbf{W}}_k \mathbf{h}_k)^{-1} \mathbf{h}_k^H (\check{\mathbf{W}}_k^{\frac{1}{2}})^H \check{\mathbf{W}}_k^{\frac{1}{2}} \mathbf{h}_k \end{aligned} \quad (55)$$

$$= \sum_{k=1}^K \varpi_k = \sum_{k=1}^K \mathbf{a}^H(\theta_B) \check{\mathbf{W}}_k \mathbf{a}(\theta_B) \quad (56)$$

$$= \mathbf{a}^H(\theta_B) (\sum_{k=1}^K \hat{\mathbf{W}}_k + \hat{\mathbf{C}}_R) \mathbf{a}(\theta_B), \quad (57)$$

where $\mathbf{A}(\theta_B) = \mathbf{a}(\theta_B) \mathbf{a}^H(\theta_B)$, $\tilde{\mathbf{A}}_k = (\check{\mathbf{W}}_k^{\frac{1}{2}})^H \mathbf{A}(\theta_B) \check{\mathbf{W}}_k^{\frac{1}{2}}$, $\varpi_k = \lambda_{\max}(\tilde{\mathbf{A}}_k)$, and (55) follows from $\varpi_k \mathbf{I}_N - \tilde{\mathbf{A}}_k \succeq 0$, and (56) is due to the rank-1 property of matrix $\tilde{\mathbf{A}}_k$. The tightness of the inequality in (55) can be achieved with $\mathbf{h}_{\text{BU},k} = 0$ and the LoS BS-IRS channel given in (12).

Hence, the proof is completed.

APPENDIX B
THE PROOF OF LEMMA 2

First, the vector \mathbf{g}_1 can be transformed as

$$\begin{aligned} \mathbf{g}_1 &= -2\text{Tr}(-\mathbf{M}_1)\text{vec}(\mathbf{e}^{(\tau)}(\mathbf{e}^{(\tau)})^H) - 2\mathbf{M}_R\text{vec}(\mathbf{e}^{(\tau)}(\mathbf{e}^{(\tau)})^H) \\ &= 2z_1\text{vec}(\mathbf{e}^{(\tau)}(\mathbf{e}^{(\tau)})^H) - 2\sum_{p=1}^{N_r}\beta_p^2\mathbf{C}_p^H\bar{\mathbf{b}}(\theta_1)\bar{\mathbf{b}}^H(\theta_1) \\ &\quad \text{vec}(\text{diag}(\mathbf{b}(\theta_p^r))\mathbf{e}^{(\tau)}(\mathbf{e}^{(\tau)})^H\text{diag}(\mathbf{b}^*(\theta_p^r))^T) \\ &= 2z_1\text{vec}(\mathbf{e}^{(\tau)}(\mathbf{e}^{(\tau)})^H) - 2\sum_{p=1}^{N_r}\beta_p^2\text{vec}(\mathbf{M}_3), \end{aligned} \quad (58)$$

where the second and third equalities are derived from the equation $\text{vec}(\mathbf{ABC}) = (\mathbf{C}^T \otimes \mathbf{A})\text{vec}(\mathbf{B})$ because \mathbf{C}_p and $\bar{\mathbf{b}}(\theta_1)$ are the Kronecker products of two matrices or vectors.

Then, by undoing the vectorization in (58), matrix \mathbf{G}_1 can be expressed as

$$\mathbf{G}_1 = 2z_1\mathbf{e}^{(\tau)}(\mathbf{e}^{(\tau)})^H - 2\sum_{p=1}^{N_r}\beta_p^2\mathbf{M}_3. \quad (59)$$

Hence, the proof is completed.

REFERENCES

- [1] F. Liu, Y. Cui, C. Masouros, J. Xu, T. X. Han, Y. C. Eldar, and S. Buzzi, "Integrated sensing and communications: Toward dual-functional wireless networks for 6G and beyond," *IEEE J. Sel. Areas Commun.*, vol. 40, no. 6, pp. 1728–1767, Mar. 2022.
- [2] F. Liu, C. Masouros, A. P. Petropulu, H. Griffiths, and L. Hanzo, "Joint radar and communication design: Applications, state-of-the-art, and the road ahead," *IEEE Trans. Commun.*, vol. 68, no. 6, pp. 3834–3862, Feb. 2020.
- [3] Y. Cui, F. Liu, X. Jing, and J. Mu, "Integrating sensing and communications for ubiquitous IoT: Applications, trends, and challenges," *IEEE Netw.*, vol. 35, no. 5, pp. 158–167, Nov. 2021.
- [4] A. Zhang, M. L. Rahman, X. Huang, Y. J. Guo, S. Chen, and R. W. Heath, "Perceptive mobile networks: Cellular networks with radio vision via joint communication and radar sensing," *IEEE Veh. Technol. Mag.*, vol. 16, no. 2, pp. 20–30, Dec. 2020.
- [5] L. Zheng, M. Lops, Y. C. Eldar, and X. Wang, "Radar and communication coexistence: An overview: A review of recent methods," *IEEE Signal Process. Mag.*, vol. 36, no. 5, pp. 85–99, Sep. 2019.
- [6] J. Li and P. Stoica, "MIMO radar with colocated antennas," *IEEE Signal Process. Mag.*, vol. 24, no. 5, pp. 106–114, Sep. 2007.
- [7] R. W. Heath, N. Gonzalez-Prelcic, S. Rangan, W. Roh, and A. M. Sayeed, "An overview of signal processing techniques for millimeter wave MIMO systems," *IEEE J. Sel. Top Signal Process.*, vol. 10, no. 3, pp. 436–453, Feb. 2016.
- [8] F. Liu, Y.-F. Liu, A. Li, C. Masouros, and Y. C. Eldar, "Cramér-raj bound optimization for joint radar-communication beamforming," *IEEE Trans. Signal Process.*, vol. 70, pp. 240–253, Dec. 2021.
- [9] F. Liu, C. Masouros, A. Li, H. Sun, and L. Hanzo, "MU-MIMO communications with MIMO radar: From co-existence to joint transmission," *IEEE Trans. Wireless Commun.*, vol. 17, no. 4, pp. 2755–2770, Feb. 2018.
- [10] Q. Wu and R. Zhang, "Intelligent reflecting surface enhanced wireless network via joint active and passive beamforming," *IEEE Trans. Wireless Commun.*, vol. 18, no. 11, pp. 5394–5409, Aug. 2019.
- [11] G. Zhou, C. Pan, H. Ren, K. Wang, and A. Nallanathan, "Intelligent reflecting surface aided multigroup multicast MISO communication systems," *IEEE Trans. Signal Process.*, vol. 68, pp. 3236–3251, Apr. 2020.
- [12] X. Song, J. Xu, F. Liu, T. X. Han, and Y. C. Eldar, "Intelligent reflecting surface enabled sensing: Cramér-raj bound optimization," 2022. [Online]. Available: <https://arxiv.org/abs/2207.05611>
- [13] X. Shao, C. You, W. Ma, X. Chen, and R. Zhang, "Target sensing with intelligent reflecting surface: Architecture and performance," *IEEE J. Sel. Areas Commun.*, vol. 40, no. 7, pp. 2070–2084, Mar. 2022.
- [14] P. Wang, W. Mei, J. Fang, and R. Zhang, "Target-mounted intelligent reflecting surface for joint location and orientation estimation," *IEEE J. Sel. Areas Commun.*, vol. 41, no. 12, pp. 3768–3782, Oct. 2023.
- [15] Z.-M. Jiang, M. Rihan, P. Zhang, L. Huang, Q. Deng, J. Zhang, and E. M. Mohamed, "Intelligent reflecting surface aided dual-function radar and communication system," *IEEE Syst. J.*, vol. 16, no. 1, pp. 475–486, Feb. 2021.
- [16] R. Liu, M. Li, Y. Liu, Q. Wu, and Q. Liu, "Joint transmit waveform and passive beamforming design for RIS-aided DFRC systems," *IEEE J. Sel. Top Signal Process.*, vol. 16, no. 5, pp. 995–1010, May. 2022.
- [17] Y.-K. Li and A. Petropulu, "Minorization-based low-complexity design for IRS-aided ISAC systems," in *2023 IEEE Radar Conference (Radar-Conf23)*. IEEE, 2023, pp. 1–6.
- [18] M. Hua, Q. Wu, C. He, S. Ma, and W. Chen, "Joint active and passive beamforming design for IRS-aided radar-communication," *IEEE Trans. Wireless Commun.*, vol. 22, no. 4, pp. 2278–2294, Oct. 2022.
- [19] H. Luo, R. Liu, M. Li, and Q. Liu, "RIS-aided integrated sensing and communication: Joint beamforming and reflection design," *IEEE Trans. Veh. Technol.*, vol. 72, no. 7, pp. 9626–9630, Feb. 2023.
- [20] Z. Xing, R. Wang, and X. Yuan, "Joint active and passive beamforming design for reconfigurable intelligent surface enabled integrated sensing and communication," *IEEE Trans. Commun.*, vol. 71, no. 4, pp. 2457–2474, Feb. 2023.
- [21] X. Zhao, H. Liu, S. Gong, X. Ju, C. Xing, and N. Zhao, "Dual-functional MIMO beamforming optimization for RIS-aided integrated sensing and communication," *IEEE Trans. Commun.*, pp. 1–1, Apr. 2024.
- [22] X. Song, X. Qin, J. Xu, and R. Zhang, "Cramér-raj bound minimization for irs-enabled multiuser integrated sensing and communications," *IEEE Trans. Wireless Commun.*, pp. 1–1, Jan. 2024.
- [23] X. Song, D. Zhao, H. Hua, T. X. Han, X. Yang, and J. Xu, "Joint transmit and reflective beamforming for IRS-assisted integrated sensing and communication," in *2022 IEEE Wireless Communications and Networking Conference (WCNC)*, 2022, pp. 189–194.
- [24] R. S. P. Sankar, S. P. Chepuri, and Y. C. Eldar, "Beamforming in integrated sensing and communication systems with reconfigurable intelligent surfaces," *IEEE Trans. Wireless Commun.*, vol. 23, no. 5, pp. 4017–4031, Sep. 2024.
- [25] C. Liao, F. Wang, and V. K. N. Lau, "Optimized design for IRS-assisted integrated sensing and communication systems in clutter environments," *IEEE Trans. Commun.*, vol. 71, no. 8, pp. 4721–4734, Jun. 2023.
- [26] M. Hua, Q. Wu, W. Chen, O. A. Dobre, and A. L. Swindlehurst, "Secure intelligent reflecting surface-aided integrated sensing and communication," *IEEE Trans. Wireless Commun.*, vol. 23, no. 1, pp. 575–591, Jun. 2024.
- [27] M. R. Bell, "Information theory and radar waveform design," *IEEE Trans. Inf. Theory*, vol. 39, no. 5, pp. 1578–1597, Sep. 1993.
- [28] B. Tang and J. Li, "Spectrally constrained MIMO radar waveform design based on mutual information," *IEEE Trans. Signal Process.*, vol. 67, no. 3, pp. 821–834, Dec. 2018.
- [29] F. Liu, Y. Xiong, K. Wan, T. X. Han, and G. Caire, "Deterministic-random tradeoff of integrated sensing and communications in gaussian channels: A rate-distortion perspective," in *2023 IEEE International Symposium on Information Theory (ISIT)*, 2023, pp. 2326–2331.
- [30] J. Li, G. Zhou, T. Gong, and N. Liu, "A framework for mutual information-based MIMO integrated sensing and communication beamforming design," *IEEE Trans. Veh. Technol.*, vol. 73, no. 6, pp. 8352–8366, Jan. 2024.
- [31] H. Zhang, "Joint waveform and phase shift design for RIS-assisted integrated sensing and communication based on mutual information," *IEEE Commun. Lett.*, vol. 26, no. 10, pp. 2317–2321, Jul. 2022.
- [32] Y. Xu, Y. Li, J. A. Zhang, M. D. Renzo, and T. Q. S. Quek, "Joint beamforming for RIS-assisted integrated sensing and communication systems," *IEEE Trans. Commun.*, vol. 72, no. 4, pp. 2232–2246, 2024.
- [33] A. M. Haimovich, R. S. Blum, and L. J. Cimini, "MIMO radar with widely separated antennas," *IEEE Signal Process. Mag.*, vol. 25, no. 1, pp. 116–129, Jan. 2007.
- [34] J. Li, G. Zhou, T. Gong, and N. Liu, "Beamforming design for active IRS-aided MIMO integrated sensing and communication systems," *IEEE Wireless Commun. Lett.*, vol. 12, no. 10, pp. 1786–1790, Jul. 2023.
- [35] X. Liu, T. Huang, N. Shlezinger, Y. Liu, J. Zhou, and Y. C. Eldar, "Joint transmit beamforming for multiuser MIMO communications and MIMO radar," *IEEE Trans. Signal Process.*, vol. 68, pp. 3929–3944, Jun. 2020.
- [36] B. Tang, M. M. Naghsh, and J. Tang, "Relative entropy-based waveform design for MIMO radar detection in the presence of clutter and interference," *IEEE Trans. Signal Process.*, vol. 63, no. 14, pp. 3783–3796, Jul. 2015.

- [37] M. A. Richards, *Fundamentals of radar signal processing*. McGraw-Hill Education, 2014.
- [38] Y. Yang and R. S. Blum, "MIMO radar waveform design based on mutual information and minimum mean-square error estimation," *IEEE Trans. Aerosp. Electron. Syst.*, vol. 43, no. 1, pp. 330–343, Jan. 2007.
- [39] X. Zhang, *Matrix analysis and applications*. Cambridge University Press, 2017.
- [40] C. Hu, L. Dai, S. Han, and X. Wang, "Two-timescale channel estimation for reconfigurable intelligent surface aided wireless communications," *IEEE Trans. Commun.*, vol. 69, no. 11, pp. 7736–7747, Apr. 2021.
- [41] Z.-Q. Luo, W.-K. Ma, A. M.-C. So, Y. Ye, and S. Zhang, "Semidefinite relaxation of quadratic optimization problems," *IEEE Signal Process. Mag.*, vol. 27, no. 3, pp. 20–34, Apr. 2010.
- [42] Y. Sun, P. Babu, and D. P. Palomar, "Majorization-minimization algorithms in signal processing, communications, and machine learning," *IEEE Trans. Signal Process.*, vol. 65, no. 3, pp. 794–816, Aug. 2016.
- [43] T. Lipp and S. Boyd, "Variations and extension of the convex–concave procedure," *Optimization and Engineering*, vol. 17, pp. 263–287, 2016.
- [44] A. Ben-Tal and A. Nemirovski, *Lectures on modern convex optimization: analysis, algorithms, and engineering applications*. SIAM, 2001.
- [45] R. A. Horn and C. R. Johnson, *Matrix analysis*. Cambridge university press, 2012.
- [46] Z. Wang, P. Babu, and D. P. Palomar, "Design of PAR-constrained sequences for MIMO channel estimation via majorization–minimization," *IEEE Trans. Signal Process.*, vol. 64, no. 23, pp. 6132–6144, Sep. 2016.
- [47] J. Gorski, F. Pfeuffer, and K. Klamroth, "Biconvex sets and optimization with biconvex functions: a survey and extensions," *Mathematical methods of operations research*, vol. 66, pp. 373–407, 2007.
- [48] W. Wu, B. Tang, and X. Wang, "Constant-modulus waveform design for dual-function radar-communication systems in the presence of clutter," *IEEE Trans. Aerosp. Electron. Syst.*, vol. 59, no. 4, pp. 4005–4017, Jan. 2023.
- [49] G. Cui, H. Li, and M. Rangaswamy, "MIMO radar waveform design with constant modulus and similarity constraints," *IEEE Trans. Signal Process.*, vol. 62, no. 2, pp. 343–353, Oct. 2014.